ABSTRACT

Master of Science Thesis

LINEAR QUADRATIC GAUSSIAN REGULATOR DESIGN FOR A HALF CAR VEHICLE MODEL

Erhan AĞIRMAN

Anadolu University
Graduate School of Sciences
Electrical and Electronics Engineering Program

Supervisor: Prof. Dr. Hüseyin AKÇAY
2007, 72 pages

This study deals with the control of active and semi-active automotive suspensions using LQG techniques. An analytical investigation of a half car model subjected to random road disturbances is performed, and the advantages of the active suspension systems, over conventional passive suspension systems are examined.

In this study in order to investigate the ride and handling characteristics of a car, a two dimensional mathematical model with a suitable road profile are developed, and the equations of motions for the proposed model with four degrees-of-freedom are derived.

The controller design is proposed to minimize the chassis and pitch angle acceleration with suspension and tire deflections when uneven road surfaces are acting on the tires of running car. Measurements from sensors located at different points of the vehicle are controller inputs and the control forces generated at each wheel of the suspension are outputs of the controller.

In the conclusion, a comparison of active suspension with LQG controller and passive suspension is made using MATLAB simulations. Simulations are performed to show that actively controlled suspensions succeeds in achieving higher levels of ride comfort and drive safety with respect to a passive setting.

Keywords: Active suspensions, LQG controller, Vehicle dynamics, One-half car model, Ride comfort

ÖZET

Yüksek Lisans Tezi

YARIM ARABA MODELİ İÇİN DOĞRUSAL GAUSYAN REGÜLATÖR TASARIMI

Erhan AĞIRMAN

Anadolu Üniversitesi
Fen Bilimleri Enstitüsü
Elektrik-Elektronik Mühendisliği Anabilim Dalı

Danışman: Prof. Dr. Hüseyin AKÇAY
2007, 72 sayfa

Bu çalışma aktif otomotiv süspansiyonlarının LQG teknikleri kullanılarak kontrolü ile ilgilidir. Tesadüfî yol gürültüsüne maruz kalan bir yarım araba modelinin analitik incelemesi yapılıp aktif süspansiyon sistemlerin geleneksel pasif olanlara göre üstünlüğü gösterilmiştir.

Bu çalışmada bir otomobilin sürüş ve kontrol karakteristiğini incelemek amacıyla aracın 2 boyutlu matematiksel modeli ile bu modele uygun yol profili oluşturuldu ve bu sistemin 4 serbestlik dereceli hareket denklemleri elde edildi.

Kontrolör tasarımı, hareket halindeki bir otomobilin tekerlekleri düz olmayan bir yol yüzeyi ile temas halindeyken kasa ve dönme açısındaki ivmelenme ile süspansiyon ve lastiklerdeki deformasyonu mümkün olduğu kadar azaltacak şekilde tasarlanmıştır. Aracın çeşitli yerlerine yerleştirilen algılayıcılardan alınan ölçümler kontrolör girdisi, süspansiyonun her bir tekerlekte üretilen kontrol gücü, kontrolörün çıktısıdır.

Sonuç olarak, MATLAB simülasyonları kullanılarak, LQG kontrolörlü aktif süspansiyon ile pasif süspansiyon karşılaştırılması yapılmıştır. Simülasyonlar, aktif olarak kontrol edilen süspansiyonun pasif yapıya göre yüksek sürüş konforu ve sürüş emniyeti sağlamada başarılı olduğunu göstermiştir.

Anahtar Kelimeler: Aktif süspansiyon, LQG kontrolör, Araç dinamiği, Yarım araba modeli, Sürüş konforu

ACKNWLEDGEMENTS

I would like to thank my supervisor Dr. Hüseyin AKÇAY for his guidance, assistance, and time in execution of this project and I also wish to thank Dr. Aydın AYBAR and Dr. Yusuf OYSAL for their reading and suggestions.

Erhan AĞIRMAN

June–2007

CONTENTS

Pages

LIST OF FIGURES

Pages

LIST OF TABLES

Pages

LIST OF ABBREVIATIONS AND SYMBOLS

A, B, C, D	: State-space matrices
DOF	: Degree of freedom
CG	: Centre of gravity
LQR	: Linear quadratic regulator
LQG	: Linear quadratic Gaussian
J	: Inertia
z	: Displacement
$\dot{z}$	: Velocity
$\ddot{z}$	: Acceleration
Q_π	: Quadratic performance index
V	: Forward speed
x	: State-vector

Subscripts

t	: Tire
f	: Front side
r	: Rear side
s	: Sprung
u	: Unsprung

1. INTRODUCTION

In recent years, automotive industry has been experiencing an increasing demand for better performance parameters such as ride comfort and good handling which are basically related with the suspension assembly of the vehicle [1].

The suspension system is responsible for isolating the vehicle from vibrations caused by unevenness of the road surface. At the same time, such a system should be able to maintain contact between the road surface and the tires to provide good vehicle handling and safety. However, a trade-off exists between these two requirements. Active suspension control systems are used in today cars because of their ability to manage the compromise between ride comfort and vehicle road-handling. In other words the purpose of active suspensions, in terms of performance, is to simultaneously improve both of these conflicting requirements.

A vehicle suspension system is the mechanism that physically separates the frame of the vehicle from the axle and wheel assemblies. It plays a major role in maintaining the tire-road contact to provide holding characteristic, minimizing the vertical acceleration transmitted to the passengers, and to keep the suspension travel small.

Basically, there are three main categories of suspension systems, namely passive, semi-active and active suspension systems. The passive suspension, which means there is no energy source in the system, includes the conventional springs and shock absorbers. Since there is no feedback control, simpler and cheaper way of suspension design is achieved.

The semi-active suspension, as the passive suspension, has no force actuator, it is possible to continuously vary the rate of energy dissipation using a controllable damper, but it is impossible to add energy.

Active suspension can supply energy from an external source which in turn creates the desired force in the suspension system to achieve the desired performance.

An actuator which is able to control its energy according to the motions of the body suspension system is located in parallel with a spring and shock absorber. The actuator is usually hydraulically controlled and applies between body and wheel a force that represents the control action generally determined with an optimization procedure.

1.1. Literature Survey

The use of active suspension on road vehicles has been considered for many years. In the last twenty years, many studies have been published on active suspension systems. Various research of control design has been done using optimal control, adaptive control methods and, H-infinity control etc. From the early 1960's optimal control theory has been used by several investigators to establish the potential benefits of the active suspension. These investigations started with simple quarter-car models, some of which include the vehicle unsprung mass consisting of a wheel and associated inertias [2]. Some extensions of the quarter-car model are half-car and full car cases which are investigated in [3, 4].

LQG approach, have been extensively used for preliminary design of active suspensions [2, 5, 6]. Chalasani (1986) presents a comprehensive analysis of full-car suspensions controlled with full-state LQG feedback. One of the studies of Hrovat (1993) is the investigation of optimal control techniques in the design of active suspensions. Thompson (1976) applied LQG full-state feedback control to an active suspension for a quarter-car model. Krtolica and Hrovat (1992) derived an analytical solution for the LQG active suspension for a simplified two degree-of-freedom half-car model.

In this study, the output feedback control for active suspension is investigated. Intention is to show the effective methodology of controller design in order to improve suspension performance especially, the heave and the pitch control as compared to simple passive suspensions.

1.2. Objective and Approach

The primary objectives of this thesis are:

1. Evaluate, both stochastic and deterministic response of the vehicle,
2. Provide a comparison between passive suspensions and the commonly used active suspensions control techniques and
3. Investigate the effectiveness of active suspensions for improving vehicle ride comfort and road handling over conventional passive counterpart.

This study presents the LQG control technique for active suspension design. It contains three main parts. In the first part, some basic topics and vocabulary which will be useful throughout the remainder of the study are introduced. The necessity of employing active suspension is discussed.

In the second part, a mathematical model of the vehicle system is introduced. State-space formulation derived and finally behavior of the passive system is discussed.

In the last part of the thesis, controller designed. Nondeterministic inputs are applied to simulate the road surface conditions more realistically. Trade-off curves are obtained. Performance analysis is performed in the time and frequency domains. The ride comfort, road handling, suspension and tire deformations are taken as performance indices; trade-offs among the various performance requirements are made using weighting curves.

In this thesis, the rms vertical acceleration of the sprung mass at the driver side is used as a measure of the vibration level, the rms suspension travel as a measure of the rattlespace requirement, and the rms tire deflection as a measure of the road handling ability.

2. THEORETICAL BACKGROUND

In this part, some basic topics related with vehicle suspension are given.

2.1. Vehicle Suspension Review

The purpose of a vehicle suspension system is to improve ride quality while maintaining good handling characteristics subject to different road profiles. Various suspension models have been used in the literature. They are named full-car, half-car, and quarter-car models according to the portion of the vehicle included in the model. Also, the suspension system is classified as a passive, semi-active, and active suspension, according to its ability to add or extract energy. This configuration is shown in figure 2.1

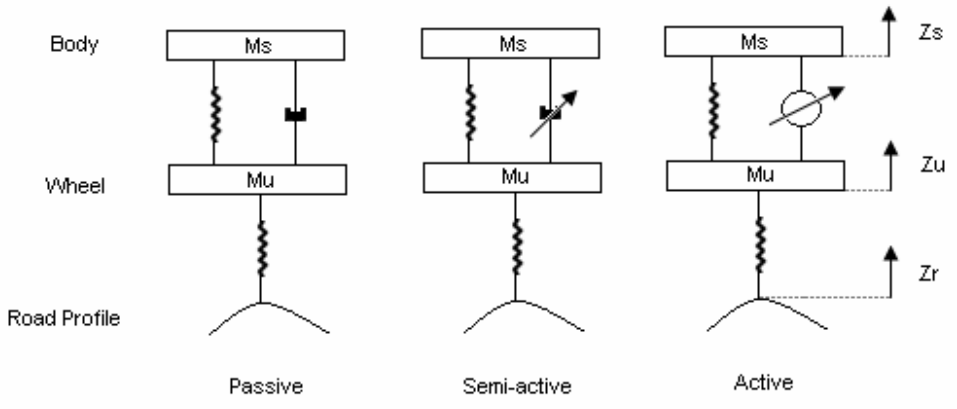

Figure 2.1. Suspension models

The conventional passive suspension system is reliable, economical and simple, but lacks adaptability to rough road environment. The active suspension system, on the other hand, is flexible and dependable, but complex and costly.

There are four important parameters which should be carefully considered in designing a vehicle suspension system [7]:

1. Ride Comfort is directly related to the acceleration sensed by passengers when traveling on a rough road.
2. Body motions which are known as bounce (heave), pitch and roll of the sprung mass are created primarily by cornering and braking maneuvers. Body motions may be present even on perfectly smooth roads.
3. Road handling is associated with the contact forces of the tires and the road surface. These contact forces create the necessary friction which prevents the tires from sliding on the road surface. The contact forces are assumed to depend linearly on the tire deflection.
4. Suspension travel refers to the relative displacement between the sprung and the unsprung masses. All suspension systems trade-offs the suspension travel for an improved ride comfort.

It is not possible to minimize all four of the above parameters at the same time with a passive suspension. The purpose of active suspensions, in terms of performance, is to simultaneously improve all of these conflicting requirements. The trade-off between passengers comfort and suspension deflection is due to the fact that is not possible to simultaneously keep both the above transfer functions small in the low frequency range. The small reduction in the vertical acceleration at low frequencies results in a large increase in the suspension deflection at these frequencies and vice versa [17].

2.2. Vocabulary and Assumptions

In this section some vocabulary are introduced in the context of the quarter car model shown in figure 2.2 These terms are used throughout the remainder of the thesis.

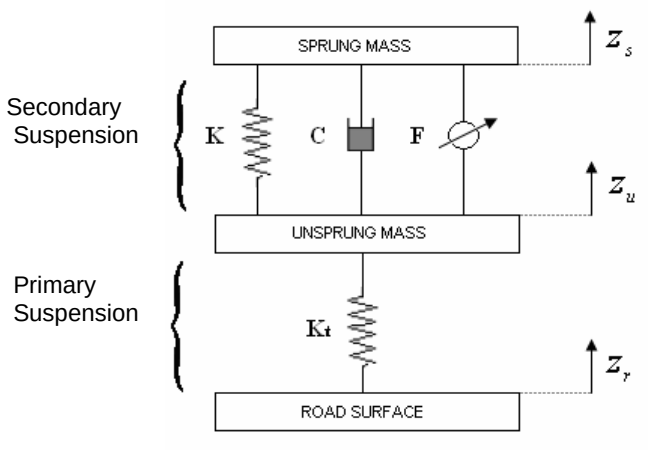

Figure 2.2. Quarter-car model

Sprung mass is a term used to describe the parts of a vehicle that are supported by the front and rear springs. They suspend the vehicle's frame, body, engine, and the power train above the wheels. The unsprung mass includes wheels, tires, brake and axle assemblies, assemblies, and other structural members not supported by the springs. A typical ratio of sprung to unsprung mass is 10:1 [10].

Unsprung mass with tire constitute primary suspension, sprung mass suspension springs and suspension dampers form secondary suspension structures. Primary suspension represents high frequency body motions (wheel hop mode) and secondary suspension represents low frequency body motions. Vehicle suspensions for road vehicles are designed to control low frequency body motions, i.e., heave and pitch in order to maintain uniform wheel to road contact. It is also important to maintain uniform contact force between the wheels and the road.

The ride quality is measured by the vertical acceleration of the vehicle body (sprung mass). The handling performance is determined by the tyre deflection, which is the difference between the wheel position and the road surface input. The controller tries to maintain a small sprung mass acceleration, while providing a large amount of damping for the unsprung mass. At low frequencies the body, which is considered to be the sprung mass portion of the vehicle, moves as an integral unit on the suspension. This is rigid body motion. The axles and the associated wheel hardware, which form the unsprung masses, also move as rigid bodies and consequently impose excitation forces on the sprung mass.

In active suspension design several assumptions are made. Otherwise some drawbacks are encountered during implementation of the system. The sprung and unsprung masses are usually considered to be rigid bodies. All suspension components are usually assumed to act on a single point of both sprung and unsprung masses. These suspension components are typically assumed to behave linearly, though some have addressed the affects of suspension nonlinearities on active suspension performance [11]. In general, suspension parameters are assumed to be invariant. Using these assumptions, the models typically used are characterized by linear time-invariant differential equations. These models, and the controllers developed for them, are discussed in the following sections.

2.3. Vehicle Coordinate System

In this part vehicle motion is described. These motions and the relative axes are shown in figure 2.3

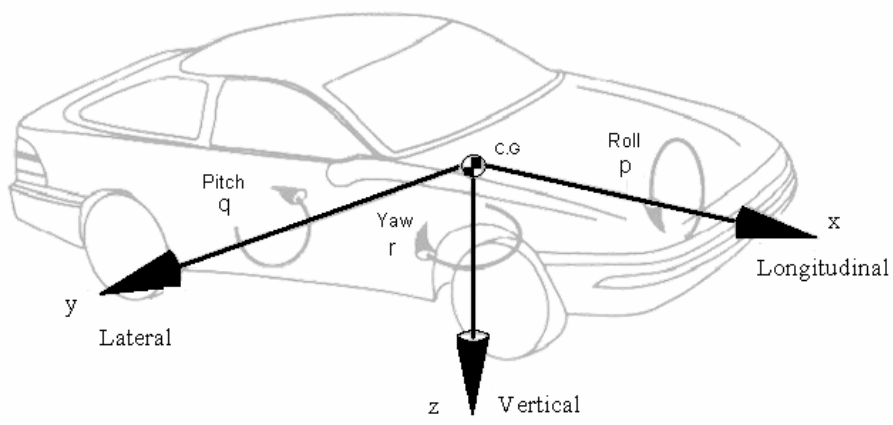

Figure 2.3. Vehicle coordinate system

The vehicle motions are defined with reference to a right-hand orthogonal coordinate system (the vehicle fixed coordinate system) which originates at the CG and travels with the vehicle. The coordinates are:

x- Forward and on the longitudinal plane of symmetry
y- Lateral out the right side of the vehicle
z- Downward with respect to the vehicle
p- Roll velocity about the x axis
q- Pitch velocity about the y axis
r- Yaw velocity about the z axis

The vertical motion of the sprung mass is referred to as heave, and is usually measured at the center of sprung mass. The rotational motion along an axis parallel to the vehicle axles is referred to as pitch. Nose-dive during vehicle braking is an example of the excitation of pitch motion.

Roll is rotational motion about an axis that spans the length of the vehicle. One roll motion excitation source is cornering. Angular motion about an axis perpendicular to the ground is called yaw. Excessive yaw results in vehicle spinout [15]. In this study half-car model is considered and therefore roll and yaw motions are never mentioned.

Another commonly used coordinate system is the ISO 8855, coordinate system; the major difference to the SAE coordinate system is that the coordinates are rotated π radians along the X-axis i.e. Z up, Y left.

Active suspension systems have also advantage of controlling the attitude of a vehicle. They can reduce the effects of braking, which causes a vehicle to nose-dive, or acceleration, which causes a vehicle to squat. They also reduce the vehicle roll during cornering maneuvers which are not included in context of this study.

2.4. Sensors

Active suspension requires sensors to be located at different points of the vehicle to continuously monitor the operating conditions of the vehicle body suspension i.e. the sprung and unsprung masses. This information is used in the online controller to command the actuator in order to provide the exact amount of force required. The control forces generated at each wheel of an active suspension are based on the sensor signals employed in the system, the forces generated at a given wheel of a passive suspension can depend only on the relative displacement and velocity at that wheel. Active suspensions may consume large amounts of energy in providing the control force and therefore in the design procedure for the active suspension the power limitations of actuators should also be considered as an important factor [7].

The selection of the places, types and number of sensors has great significance in controlled suspension systems. The sensor configuration should be capable of providing enough information about each wheel's motion as well as the car body's dynamic behavior. In addition, sensors mounted at each wheel hub provide the estimator sufficient information about the road disturbances.

The selection of actuators and sensors can limit the bandwidth of the system, regardless of the controller type "Van de Wal and de Jager, (1996)". Most of the controller types used in automotive applications requires full state feedback [8] as is also the case in this study. It should be noted that vertical acceleration of the CG has been utilized by some researchers as a key parameter in optimal ride control systems [9].

2.5. Road Surface Roughness

The road profile is usually considered to be a random process $z(l)$, where z is the road height and l is the distance along the road. As the vehicle travels along the road with velocity v, the random process $z(l)$ is converted to a random process $x(t)$ which is input to the vehicle suspension via the tyre. The random process $x(t)$ is usually described in terms of its power spectral density as a function of frequency in either radians or cycles per unit distance. In this study a real road surface taken as a random exciting function is used as the road input to the system.

If all road surfaces were smooth enough, there would be no need using suspension systems in vehicles since no vertical excitations forces would be impacting to them. There would be no vibration from which to isolate the passenger. But in real World, roads are not nice and smooth due to construction limitations and also due to road surface deterioration over time. This road roughness is the ultimate input to the mechanical system under consideration, and so necessity and importance of the suspension arises.

Disturbance from the roughness of the road is the most important parameter in considering ride quality. In order to simulate vehicle vibration behavior for the purposes of calculating dynamic tyre forces or ride performance, it is necessary to assume a road roughness input

Road disturbances can be classified in many ways but there is two main classes that are vibration and shock. Shock is described by a relatively short duration, high intensity event, such as a pothole or speedbump.

Vibration is characterized by prolonged, relatively consistent low amplitude, excitations, the typical “road roughness”, [4]. And it is also important that a suspension system must provide enough ride quality with both types of road conditions, in addition to any handling requirements during turning, breaking and acceleration.

An appropriate analysis of the ride performance limitations of suspension systems requires detailed road modeling analysis. In the past, for the vehicles, simple functions such as step functions, sine waves, or triangular waves were generally used as disturbances from the ground. While these inputs provide a basic idea for comparative evaluation of designs, it is recognized that the road surface is usually not represented by these simple functions, and therefore the deterministic irregular shapes cannot serve as a valid basis for studying the actual behaviors of the vehicle. Thus, it is important to predict vehicle dynamics response using realistic road model [7].

2.6. Vibration Isolation

Vibration in a vehicle is very undesirable because it can cause discomfort to the passengers in the vehicle. Vibration is undesirable, not only because of the unpleasant motion, the noise and the dynamic stresses, which may lead to failure of the structure, but also because of the energy losses and the reduction in performance which accompany the vibrations [14].

Certain vibration inputs to the human body can even cause disorders. The research results have proven that a zone or area can be defined in which people generally experience discomfort. Above this region the vibration is certain to be intolerable, and below this region the vibration level is acceptable.

There are three main standards by which whole-body vibration health risks are measured. ISO 2631-5:2004 addresses human exposure to mechanical multiple shocks measured at the seat pad when a person is seated.

ISO2631-74, 85 proposes sensitivity curves for each axis over a range of frequencies from 1−80 Hz. The curve for the z-axis, which is the primary concern here, shows greatest sensitivity in the 4 - 8 Hz range. Above 8 Hz the sensitivity increases proportionally with respect to frequency. Below 4 Hz, the sensitivity is inversely proportional to the square root of frequency. Humans are most tolerant of high frequency vibration, yet the magnitude of the road inputs falls of with increasing frequency. These curves are generally used to estimate the level of health hazard present given a particular magnitude and duration of vibration [15].

3. VEHICLE MODEL AND DYNAMICS

This part is devoted to the mathematical modeling of vehicle, considering the road disturbance. First a two dimensional half-vehicle model will be introduced, its equations of motion will be derived, and a representative state space system will be defined and used for the remainder of this study. Once the model is established, it can be used to investigate vehicle dynamics for various disturbances.

3.1. Half-Vehicle Model

The well-known rigid half-car vehicle model, which is shown in figure 3.1, is widely used for active suspension design. Since the angular motion of the vehicle is not captured in the quarter car model and the one degree-of-freedom model does not account for the dynamical effects of the unsprung mass (wheelhop dynamics) a half vehicle model was chosen for this work. It is also possible to make a more realistic analysis compared with the quarter-car model.

A linear model is considered to represent the road vehicle dynamics. The model consists of three masses. While the top mass, M_s , represents the vehicle body, the two lower masses, m_{uf} and m_{ur} , represent the front and rear tires respectively. Body motions are considered to be heave and pitch. In order to obtain a linear model, pitch angle is assumed to be small.

The suspension system is modelled by two linear springs in parallel with two viscous dampers and for each tire a single spring is used. The suspension system connects the sprung mass to the two unsprung masses which are free to bounce vertically with respect to the sprung mass. The actuators are considered to be a source of controllable force and located parallel with the suspension springs and dampers.

The system with four degrees of freedom is represented by the body bounce (heave), z_s; body pitch, θ and the tire deflections, z_{uf}, z_{ur}. The system as a whole is moving at a constant horizontal speed. The rest of the variables are considered time-varying functions.

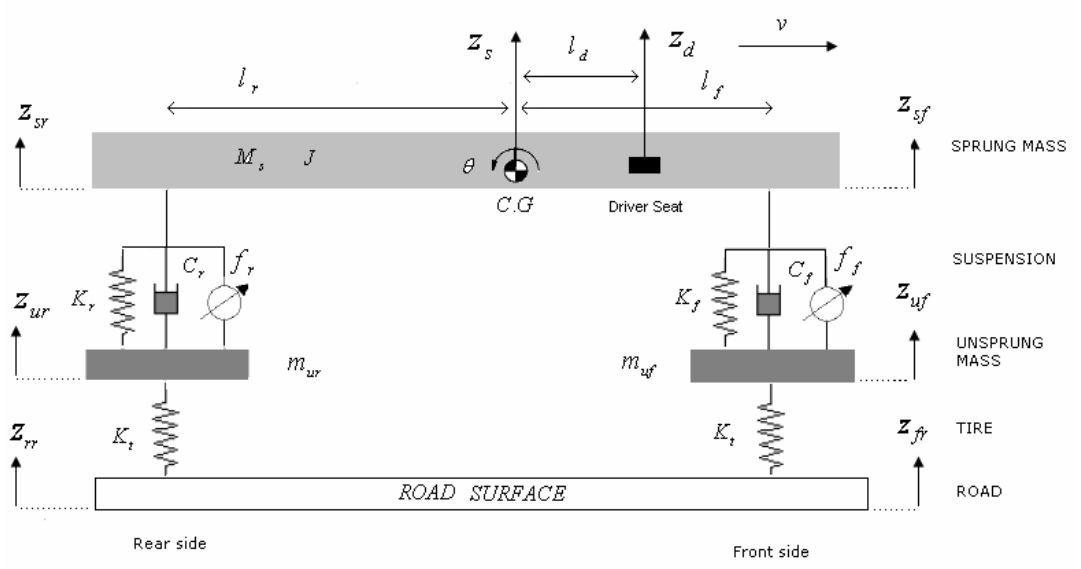

Figure 3.1. 4-DOF half-car model

3.2. Equations of Motion

An automobile suspension system is modelled as a system of 8th-order ordinary differential equations (ODEs) that are derived from the Newton's 2nd law of motion:

$$force = mass\ x\ \ acceleration$$

The following motion equations could be derived using Newton-Euler method. The force equilibrium equation for the sprung mass in the vertical direction can be written as

$$\begin{aligned} M_s \ddot{z}_s = &-f_f - f_r - K_f(z_{sf} - z_{uf}) - K_r(z_{sr} - z_{ur}) \\ &- C_f(\dot{z}_{sf} - \dot{z}_{uf}) - C_r(\dot{z}_{sr} - \dot{z}_{ur}) \end{aligned} \quad (3.1)$$

the moment equation for the pitching motion about the C.G. can be expressed as

$$J\ddot{\theta} = l_r[f_r + K_r(z_{sr} - z_{ur}) + C_r(\dot{z}_{sr} - \dot{z}_{ur})]$$

$$- l_f[f_f + K_f(z_{sf} - z_{uf}) + C_f(\dot{z}_{sf} - \dot{z}_{uf})] \qquad (3.2)$$

and the force equilibrium equation for the unsprung masses:

$$m_{uf}\ddot{z}_{uf} = f_f - K_t(z_{uf} - z_{fr}) + K_f(z_{sf} - z_{uf}) + C_f(\dot{z}_{sf} - \dot{z}_{uf}) \qquad (3.3)$$

$$m_{ur}\ddot{z}_{ur} = f_r - K_t(z_{ur} - z_{rr}) + K_r(z_{sr} - z_{ur}) + C_r(\dot{z}_{sr} - \dot{z}_{ur}) \qquad (3.4)$$

The following kinematics relations are easily derived under the assumption of the linearity.

$$z_{sf} = z_s + l_f\theta \qquad (3.5)$$

$$z_{sr} = z_s - l_r\theta \qquad (3.6)$$

$$\dot{z}_{sf} = \dot{z}_s + l_f\dot{\theta} \qquad (3.7)$$

$$\dot{z}_{sr} = \dot{z}_s - l_r\dot{\theta} \qquad (3.8)$$

$$z_d = z_s + l_r\theta \qquad (3.9)$$

Plugging (3.5)-(3.9) into the (3.1)-(3.4):

$$M_s\ddot{z}_s = -f_f - f_r - K_f(z_s + l_f\theta - z_{uf}) - K_r(z_s - l_r\theta - z_{ur})$$

$$- C_f(\dot{z}_s + l_f\dot{\theta} - \dot{z}_{uf}) - C_r(\dot{z}_s - l_r\dot{\theta} - \dot{z}_{ur}) \qquad (3.10)$$

$$J\ddot{\theta} = l_r[f_r + K_r(z_s - l_r\theta - z_{ur}) + C_r(\dot{z}_s - l_r\dot{\theta} - \dot{z}_{ur})]$$

$$- l_f[f_f + K_f(z_s + l_f\theta - z_{uf}) + C_f(\dot{z}_s + l_f\dot{\theta} - \dot{z}_{uf})] \qquad (3.11)$$

$$m_{uf}\ddot{z}_{uf} = f_f - K_t(z_{uf} - z_{fr}) + K_f(z_s + l_f\theta - z_{uf}) + C_f(\dot{z}_s + l_f\dot{\theta} - \dot{z}_{uf}) \quad (3.12)$$

$$m_{ur}\ddot{z}_{ur} = f_r - K_t(z_{ur} - z_{rr}) + K_r(z_s - l_r\theta - z_{ur}) + C_r(\dot{z}_s - l_r\dot{\theta} - \dot{z}_{ur}) \quad (3.13)$$

Note that the gravity force is not considered in the equations, as the displacement of the body is considered from the static equilibrium position. Hence the spring force due to the initial compression of the spring balances the gravity force.

Rewriting (3.10)-(3.13) in such a way that the system matrices can be written easily:

$$M_s\ddot{z}_s = -(K_f + K_r)z_s - (l_fK_f - l_rK_r)\theta + K_f z_{uf} + K_r z_{ur} - (C_f + C_r)\dot{z}_s - (l_fC_f - l_rK_r)\dot{\theta} + C_f\dot{z}_{uf} + C_r\dot{z}_{ur} - f_f - f_r \quad (3.14)$$

$$J\ddot{\theta} = -(l_fK_f - l_rK_r)z_s - (l_f{}^2K_f + l_r{}^2K_r)\theta + l_fK_f z_{uf} - l_rK_r z_{ur} - (l_fC_f - l_rC_r)\dot{z}_s - (l_f{}^2C_f + l_r{}^2C_r)\dot{\theta} + l_fC_f\dot{z}_{uf} - l_rC_r\dot{z}_{ur} - l_f f_f + l_r f_r \quad (3.15)$$

$$m_{uf}\ddot{z}_{uf} = K_f z_s + l_fK_f\theta - (K_f + K_r)z_{uf} + C_f\dot{z}_s + l_fC_f\dot{\theta} - C_f\dot{z}_{uf} + K_t z_{fr} + f_f \quad (3.16)$$

$$m_{ur}\ddot{z}_{ur} = K_r z_s - l_rK_r\theta - (K_r + K_t)z_{ur} + C_r\dot{z}_s - l_rC_r\dot{\theta} - C_r\dot{z}_{ur} + K_t z_{rr} + f_r \quad (3.17)$$

The variables used to represent the vehicle components in the model are shown in Table 3.1 and the displacement components of the vehicle states are described in Table 3.2. The parameters related to the unsprung masses are denoted with subscript u while the sprung mass parameters have subscript s.

Table 3.1. Vehicle model parameter definitions

Symbols	Descriptions	Units
C_{s1}	Front suspension damper	Ns/m
C_{s2}	Rear suspension damper	Ns/m
K_f	Front suspension stiffness	N/m
K_r	Rear suspension stiffness	N/m
K_t	Front and rear tires stiffness	N/m
M_s	Vehicle sprung mass	kg
J	Pitch moment of inertia of the sprung mass	kg. m^2
m_{uf}	Front unsprung mass	kg
m_{ur}	Rear unsprung mass	kg
l_f	Longitudinal distance from center of mass to Front suspension attachment point	m
l_r	Longitudinal distance from center of mass to rear suspension attachment point	m
l_d	Longitudinal distance from center of mass to driver seat point	m

Table 3.2. Vehicle model states

Symbols	Descriptions	Units
z_s	Sprung Mass C.G Vertical Displacement	m
z_d	Sprung Mass Driver Seat Vertical Displacement	m
z_{sf}	Vertical Displacement of Sprung Mass at Front Suspension Attachment Point	m
z_{sr}	Vertical Displacement of Sprung Mass at Rear Suspension Attachment Point	m
z_{uf}	Front Unsprung Mass Vertical Displacement	m
z_{ur}	Rear Unsprung Mass Vertical Displacement	m
z_f	Vertical Displacement of Road at Front Axle	m
z_r	Vertical Displacement of Road at Rear Axle	m
θ	Sprung Mass Pitch Angle	rad/s

3.3. State-Space Model

For the computer simulation it is difficult to work with the differential equations. Therefore, motion equations of the system must be placed into a state space form. This transformation is as follows:

First displacement, actuator and disturbance vectors are defined as

$$\psi = \begin{bmatrix} z_s \\ \theta \\ z_{uf} \\ z_{ur} \end{bmatrix},\ u = \begin{bmatrix} f_f \\ f_r \end{bmatrix} \text{ and } w = \begin{bmatrix} z_f \\ z_r \end{bmatrix} \tag{3.18}$$

then (3.14) through (3.17) can be written by using the vectors and their derivatives defined in (3.18)

$$M\begin{bmatrix} \ddot{z}_s \\ \ddot{\theta} \\ \ddot{z}_{uf} \\ \ddot{z}_{ur} \end{bmatrix} = -K\begin{bmatrix} z_s \\ \theta \\ z_{uf} \\ z_{ur} \end{bmatrix} - C\begin{bmatrix} \dot{z}_s \\ \dot{\theta} \\ \dot{z}_{uf} \\ \dot{z}_{ur} \end{bmatrix} + F\begin{bmatrix} f_f \\ f_r \end{bmatrix} + Z\begin{bmatrix} z_f \\ z_r \end{bmatrix} \tag{3.19}$$

or more compactly

$$M\ddot{\psi} + C\dot{\psi} + K\psi = Fu + Zw \tag{3.20}$$

where the matrices M, C and K are the mass, damping, and stiffness matrices, respectively and w is the disturbance vector arising from the ground displacement and F and Z are constant matrices with appropriate dimensions. These matrices can be easily derived as follows.

$$M = \begin{bmatrix} M_s & 0 & 0 & 0 \\ 0 & J & 0 & 0 \\ 0 & 0 & m_{uf} & 0 \\ 0 & 0 & 0 & m_{ur} \end{bmatrix},$$

$$K = \begin{bmatrix} K_f + K_r & l_f K_f - l_r K_r & -K_f & -K_r \\ l_f K_f - l_r K_r & l_f{}^2 K_f + l_r{}^2 K_r & -l_f K_f & l_r K_r \\ -K_f & -l_f K_f & K_f + K_t & 0 \\ -K_r & l_r K_r & 0 & K_r + K_t \end{bmatrix},$$

$$C = \begin{bmatrix} C_f + C_r & l_f C_f - l_r C_r & -C_f & -C_r \\ l_f C_f - l_r C_r & l_f{}^2 C_f + l_r{}^2 C_r & -l_f C_f & l_r C_r \\ -C_f & -l_f C_f & C_f & 0 \\ -C_r & l_r C_r & 0 & C_r \end{bmatrix}, \text{ and}$$

$$F = \begin{bmatrix} -1 & -1 \\ -l_f & l_r \\ 1 & 0 \\ 0 & 1 \end{bmatrix}, \quad Z = \begin{bmatrix} 0 & 0 \\ 0 & 0 \\ K_t & 0 \\ 0 & K_t \end{bmatrix}$$

Rewriting (3.20)

$$\ddot{\psi} = -M^{-1} C \dot{\psi} - M^{-1} K \psi + M^{-1} F u + M^{-1} Z w \tag{3.21}$$

Defining the state variables x as

$$x = \begin{bmatrix} \psi \\ \dot{\psi} \end{bmatrix} \tag{3.22}$$

then,

$$\dot{\psi} = [0_{4x4} \quad I_4] x \tag{3.23}$$

Where I is the identity matrix and finally,

$$\ddot{\psi} = \begin{bmatrix} -M^{-1} K & -M^{-1} C \end{bmatrix} x + M^{-1} F u + M^{-1} Z w \tag{3.24}$$

These equations could be simply written as a matrix equation by using (3.23) and (3.24) in (3.22):

$$\dot{x} = Ax + B_1 w + B_2 u \tag{3.25}$$

where

$$A = \begin{bmatrix} 0_{4x4} & I_4 \\ -M^{-1}K & -M^{-1}C \end{bmatrix},\ B_1 = \begin{bmatrix} 0_{4x2} \\ M^{-1}Z \end{bmatrix}, \text{ and } B_2 = \begin{bmatrix} 0_{4x2} \\ M^{-1}F \end{bmatrix} u$$

and the states used to make these transformations are defined as:

$$x = \begin{bmatrix} z_s \\ \theta \\ z_{uf} \\ z_{ur} \\ \dot{z}_s \\ \dot{\theta} \\ \dot{z}_{uf} \\ \dot{z}_{ur} \end{bmatrix} \begin{array}{l} \text{Heave displacement} \\ \text{Pitch angle} \\ \text{Front wheel displacement} \\ \text{Rear wheel displacement} \\ \text{Heave velocity} \\ \text{Pitch angular velocity} \\ \text{Front wheel velocity} \\ \text{Rear wheel velocity} \end{array} \tag{3.26}$$

3.3.1. Regulated outputs

The vector of regulated outputs can be written with the relative displacements and velocities at the suspension connections as a linear combination of the state disturbances and inputs; that is,

$$z = \begin{bmatrix} \ddot{z}_d \\ \ddot{\theta} \\ z_{sf} - z_{uf} \\ z_{sr} - z_{ur} \\ z_{uf} - z_{fr} \\ z_{ur} - z_{rr} \end{bmatrix} \begin{array}{l} \text{Heave acceleration} \\ \text{Pitch angle acceleration} \\ \text{Front suspension deflection} \\ \text{Rear suspension deflection} \\ \text{Front tire deflection} \\ \text{Rear tire deflection} \end{array} \tag{3.27}$$

Each component of z is written in terms of state input, controlled input and road input vectors as follows:

$$\ddot{z}_s = [1 \quad 0 \quad 0 \quad 0]\ddot{\psi}$$

$$= [1 \quad 0 \quad 0 \quad 0]\{[-M^{-1}K \quad -M^{-1}C]x + M^{-1}Fu + M^{-1}Zw\}$$

$$= [1 \quad 0 \quad 0 \quad 0][-M^{-1}K \quad -M^{-1}C]x + [1 \quad 0 \quad 0 \quad 0]M^{-1}Fu$$

$$+ [1 \quad 0 \quad 0 \quad 0]M^{-1}Zw$$

$$= \gamma_1 x + \gamma_2 u + \gamma_3 w \tag{3.28}$$

$$\ddot{\theta} = [0 \quad 1 \quad 0 \quad 0]\ddot{\psi}$$

$$= [0 \quad 1 \quad 0 \quad 0]\{[-M^{-1}K \quad -M^{-1}C]x + M^{-1}Fu + M^{-1}Zw\}$$

$$= [0 \quad 1 \quad 0 \quad 0][-M^{-1}K \quad -M^{-1}C]x + [0 \quad 1 \quad 0 \quad 0]M^{-1}Fu$$

$$+ [0 \quad 1 \quad 0 \quad 0]M^{-1}Zw$$

$$= \beta_1 x + \beta_2 u + \beta_3 w \tag{3.29}$$

$$\ddot{z}_d = \ddot{z}_s + l_d\ddot{\theta} = [1 \quad l_d \quad 0 \quad 0]\ddot{\psi}$$

$$= [1 \quad l_d \quad 0 \quad 0]\{[-M^{-1}K \quad -M^{-1}C]x + M^{-1}Fu + M^{-1}Zw\}$$

$$= [1 \quad l_d \quad 0 \quad 0][-M^{-1}K \quad -M^{-1}C]x + [1 \quad l_d \quad 0 \quad 0]M^{-1}Fu$$

$$+ [1 \quad l_d \quad 0 \quad 0]M^{-1}Zw$$

$$= \alpha_1 x + \alpha_2 u + \alpha_3 w \tag{3.30}$$

$$z_{sf} - z_{uf} = z_s + l_f\theta - z_{uf} = [1 \quad l_f \quad -1 \quad 0 \quad 0_{1x4}]x \tag{3.31}$$

$$z_{sr} - z_{ur} = z_s - l_r\theta - z_{ur} = [1 \quad -l_r \quad 0 \quad -1 \quad 0_{1x4}]x \tag{3.32}$$

$$z_{uf} - z_{fr} = [0 \quad 0 \quad 1 \quad 0 \quad 0_{1x4}]x - w_1 \tag{3.33}$$

$$z_{ur} - z_{rr} = [0 \quad 0 \quad 0 \quad 1 \quad 0_{1x4}]x - w_2 \tag{3.34}$$

Equations (3.28)-(3.34) could be simply written as a matrix equation as

$$z = C_1 x + D_{11} w + D_{12} u \tag{3.35}$$

where

$$C_1 = \begin{bmatrix} \alpha_1 & & & & & & & \\ \beta_1 & & & & & & & \\ 1 & l_f & -1 & 0 & 0 & 0 & 0 & 0 \\ 1 & -l_r & 0 & -1 & 0 & 0 & 0 & 0 \\ 0 & 0 & 1 & 0 & 0 & 0 & 0 & 0 \\ 0 & 0 & 0 & 1 & 0 & 0 & 0 & 0 \end{bmatrix}, \; D_{11} = \begin{bmatrix} \alpha_3 & \\ \beta_3 & \\ 0 & 0 \\ 0 & 0 \\ -1 & 0 \\ 0 & -1 \end{bmatrix} \text{ and } \; D_{12} = \begin{bmatrix} \alpha_2 & \\ \beta_2 & \\ 0 & 0 \\ 0 & 0 \\ 0 & 0 \\ 0 & 0 \end{bmatrix}$$

3.3.2. Output measurements for the feedback purpose

As in the previous case, the vector of measured outputs can be written with the relative displacements and velocities at the suspension connections as a linear combination of the states, disturbances, and inputs; that is,

$$y = \begin{bmatrix} \ddot{z}_{sf} \\ \ddot{z}_{sr} \\ \ddot{z}_{uf} \\ \ddot{z}_{ur} \\ z_{sf} - z_{uf} \\ z_{sr} - z_{ur} \\ z_{uf} \\ z_{ur} \end{bmatrix} \begin{matrix} \text{Sprung mass front end acceleration} \\ \text{Sprung mass rear end acceleration} \\ \text{Front wheel acceleration} \\ \text{Rear wheel acceleration} \\ \text{Front suspension stroke} \\ \text{Rear suspension stroke} \\ \text{Front wheel displacement} \\ \text{Rear wheel displacement} \end{matrix} \tag{3.36}$$

They are assumed to be available.

Like as in (3.35), each component of y is written in terms of state input, controlled input and road input vectors and these equations could be simply written as a matrix equation.

$$y = C_2 x + D_{21} w + D_{22} u \tag{3.37}$$

and the matrices C_2, D_{21} and D_{22} can be observed from (3.5)-(3.8), (3.12), (3.13) and (3.28)-(3.32)

$$C_2 = \begin{bmatrix} \gamma_1 + l_f\beta_1 & & & & & & & \\ \gamma_1 - l_r\beta_1 & & & & & & & \\ \frac{K_f}{m_{uf}} & \frac{l_f K_f}{m_{uf}} & \frac{-K_t - K_f}{m_{uf}} & 0 & \frac{C_f}{m_{uf}} & \frac{l_f C_f}{m_{uf}} & \frac{-C_f}{m_{uf}} & 0 \\ \frac{K_r}{m_{ur}} & \frac{-l_r K_r}{m_{ur}} & 0 & \frac{-K_t - K_r}{m_{ur}} & \frac{C_r}{m_{ur}} & \frac{-l_r C_r}{m_{ur}} & 0 & \frac{-C_r}{m_{ur}} \\ 1 & l_f & -1 & 0 & 0 & 0 & 0 & 0 \\ 1 & -l_r & 0 & -1 & 0 & 0 & 0 & 0 \\ 0 & 0 & 1 & 0 & 0 & 0 & 0 & 0 \\ 0 & 0 & 0 & 1 & 0 & 0 & 0 & 0 \end{bmatrix},$$

$$D_{21} = \begin{bmatrix} \gamma_3 + l_f\beta_3 & \\ \gamma_3 - l_r\beta_3 & \\ \frac{K_t}{m_{uf}} & 0 \\ 0 & \frac{K_t}{m_{ur}} \\ 0 & 0 \\ 0 & 0 \\ 0 & 0 \\ 0 & 0 \end{bmatrix}, \text{ and } D_{22} = \begin{bmatrix} \gamma_2 + l_f\beta_2 & \\ \gamma_2 - l_r\beta_2 & \\ \frac{1}{m_{uf}} & 0 \\ 0 & \frac{1}{m_{ur}} \\ 0 & 0 \\ 0 & 0 \\ 0 & 0 \\ 0 & 0 \end{bmatrix}$$

and finally by combining (3.25), (3.35) and (3.37) state-space formulation of the vehicle system with regulated outputs is obtained as

$$\begin{aligned} \dot{x} &= Ax + B_1 w + B_2 u \\ z &= C_1 x + D_{11} w + D_{12} u \\ y &= C_2 x + D_{21} w + D_{22} u \end{aligned} \tag{3.38}$$

In summary,

State vector:

$$x = \begin{bmatrix} z_s & \theta & z_{uf} & z_{ur} & \dot{z}_s & \dot{\theta} & \dot{z}_{uf} & \dot{z}_{ur} \end{bmatrix}^T$$

Regulated output vector:

$$z = \begin{bmatrix} \ddot{z}_d & \ddot{\theta} & z_{sf} - z_{uf} & z_{sr} - z_{ur} & z_{uf} - z_{rf} & z_{ur} - z_{rr} \end{bmatrix}^T$$

Measured output vector

$$y = \begin{bmatrix} \ddot{z}_{sf} & \ddot{z}_{sr} & \ddot{z}_{uf} & \ddot{z}_{ur} & z_{sf} - z_{uf} & z_{sr} - z_{ur} & z_{uf} & z_{ur} \end{bmatrix}^T$$

Road input vector (process noise):

$$w = \begin{bmatrix} z_f & z_r \end{bmatrix}^T$$

Controlled input vector (measured noise):

$$u = \begin{bmatrix} f_f & f_r \end{bmatrix}^T$$

Equation (3.38) represents the state-space formulation of the half-car vehicle system without a reference to a disturbance model included to the system. In the following section, the disturbance model will be defined and appended to the system.

3.4. Disturbance Modeling

In control systems disturbance rejection is often more important. Feedback control is necessary to reduce the effect of these disturbances. Therefore feedback configuration must compromise the disturbance inputs and the dynamic properties of the disturbance must be estimated, modeled and included in the controller design.

In this study it is assumed that only ride input is allowed. It means that there are no braking and acceleration inputs.

3.4.1. Colored noise displacement input

It is not possible to measure road disturbances exactly. Therefore an estimated road model must be utilized to combine the road inputs with the vehicle model. The disturbance to a vehicle can be modelled as a zero-mean colored stochastic process. The ride input is described by a shape filter such that a zero-mean white noise source v at the input to the filter produces an appropriately time correlated stochastic ride disturbance w at the output. Modeling colored noise displacement input let

$$\begin{aligned} \dot{Z}(l) &= A_v Z(l) + B_v v(l) \\ \xi(l) &= C_v Z(l) + D_v v(l) \end{aligned} \tag{3.39}$$

Where $\xi(t)$ denotes the road displacement at the longitudinal coordinate l and $v(l)$ is a zero mean (spatial) white noise process with a covariance function:

$$E\{v(l)v(l+\tau)\} = R_v(\tau) = \delta(\tau) \tag{3.40}$$

In the design of a linear shape filter, one aims to match given spectral data as closely possible as by suitably selecting the state-space parameters (A_v, B_v, C_v) in (3.39). Note that the shaping filter required to describe typical ride inputs is in the form of a low-pass filter $(D_v = 0)$, usually of first or second order. A block diagram of such a shape filter is shown in figure 3.2

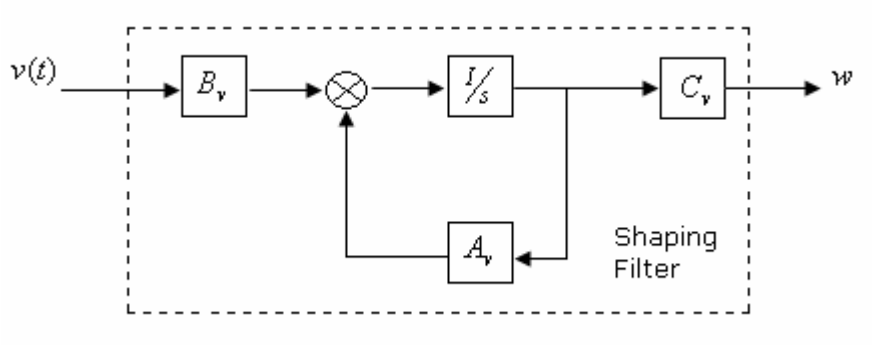

Figure 3.2. Ride input generation by filtering white noise

Applying the chain rule of differentiation to $l = vt$ and (3.39) can be transformed into the time domain as follows:

$$\begin{aligned} \dot{x}_v(t) &= vA_v x_v(t) + \sqrt{v}B_v v(t), \\ w(t) &= C_v x_v(t), \end{aligned}$$

or more compactly

$$\begin{aligned} \dot{x}_v(t) &= A_w x_v(t) + B_w v(t), \\ w(t) &= C_w x_v(t), \end{aligned} \tag{3.41}$$

with $\dim(x_v) = n_v$

Outputs of the shape filter are derived from the measurements of the road profile power spectrum by an identification algorithm [13] and filter parameters are written below.

$$A_w = \begin{bmatrix} -10.0420 & -0.6481 \\ 0.6481 & 0 \end{bmatrix},\ B_w = \begin{bmatrix} 1 \\ 0 \end{bmatrix},$$

$$C_w = \begin{bmatrix} 0 & 0.1809 \end{bmatrix}, \text{ and } D_w = 0$$

In (3.41), $x_v(t) = Z(vt), w(t) = \xi(vt),$ and $v(t)$ is a zero-mean (temporal) white noise process with a covariance function $R_{n(t)}(\tau) = \delta(t)$. Remember that vehicle forward velocity is denoted by v. Also note that this ride disturbance w acts as the input to the vehicle system.

Plugging w from (3.41) into (3.38):

$$\begin{aligned} \dot{x} &= Ax + B_1 C_w x_v + B_2 u \\ z &= C_1 x + D_{11} C_w x_v + D_{12} u \\ y &= C_2 x + D_{21} C_w x_v + D_{22} u \end{aligned} \tag{3.42}$$

State-space formulation of the system can be rewritten by forming an augmented state vector:

$$\widetilde{x} = \begin{bmatrix} \dot{x} \\ \dot{x}_v \end{bmatrix} \tag{3.43}$$

including the system states x and the disturbance state x_v. The augmented state-space model of the system is then

$$\dot{\widetilde{x}} = \begin{bmatrix} A & B_1 C_w \\ 0 & A_w \end{bmatrix} \widetilde{x} + \begin{bmatrix} 0 \\ B_w \end{bmatrix} \nu + \begin{bmatrix} B_2 \\ 0 \end{bmatrix} u$$

$$z = \begin{bmatrix} C_1 & D_{11} C_w \end{bmatrix} \widetilde{x} + D_{12} u \tag{3.44}$$

$$y = \begin{bmatrix} C_2 & D_{21} C_w \end{bmatrix} \widetilde{x} + D_{22} u$$

or compactly

$$\begin{aligned} \dot{\widetilde{x}} &= \widetilde{A}\widetilde{x} + \widetilde{B}_1 \nu + \widetilde{B}_2 u \\ \widetilde{z} &= \widetilde{C}_1 \widetilde{x} + D_{12} u \\ \widetilde{y} &= \widetilde{C}_2 \widetilde{x} + D_{22} u \end{aligned} \tag{3.45}$$

where

$$\widetilde{A} = \begin{bmatrix} A & B_1 C_w \\ 0 & A_w \end{bmatrix}, \ \widetilde{B}_1 = \begin{bmatrix} 0 \\ B_w \end{bmatrix}, \ \widetilde{B}_2 = \begin{bmatrix} B_2 \\ 0 \end{bmatrix}$$

$$\widetilde{C}_1 = \begin{bmatrix} C_1 & D_{11} C_w \end{bmatrix}, \text{ and } \widetilde{C}_2 = \begin{bmatrix} C_2 & D_{21} C_w \end{bmatrix}$$

Equation (3.44) describes the combined vehicle model and the road model. Simplified form of (3.44) is written as (3.45).

3.4.2. Pothole input

In this thesis, two kinds of road excitation inputs, including random and pothole excitations are used for simulation of suspension system. The former one is explained in the previous section. The response of a vehicle to a pothole road input is discussed in this section.

Random input is used for smooth road in order to evaluate ride comfort. On the other hand, pothole input is used for rough road modeling where handling is major concern. Pothole input offers a large amplitude excitation and they are usually characterized as a half-sine wave input. But in this case, a 0.08 m depth and 0.5 m length rectangle is used. The configuration of pothole excitation is shown in figure 3.3. Note that the rear vehicle input is a delayed version of that at the front wheel. This delay is equal to

$$\tau = \frac{l_f + l_r}{v} \tag{3.46}$$

where $l_f + l_r$ is the vehicle wheelbase and v is vehicle forward velocity.

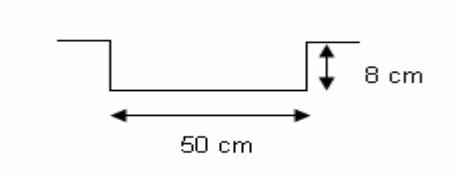

(a) Geometric representation

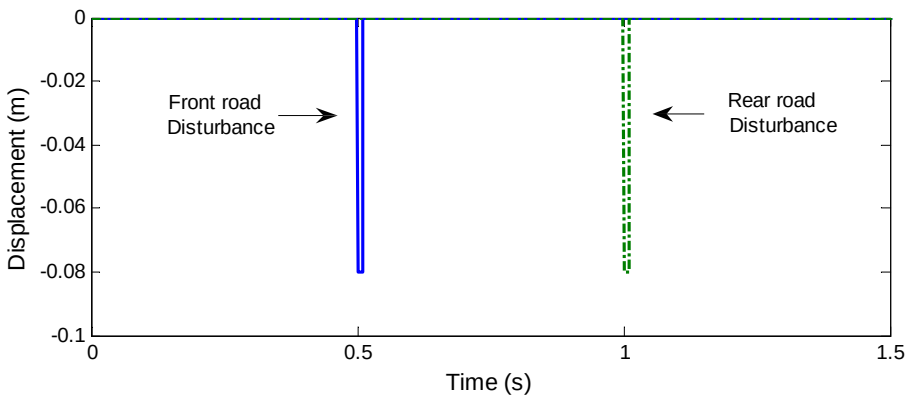

(b) Time domain representation

Figure 3.3. Pothole road disturbance @ v=8 m/s

The main principle of using potholes is to introduce shocks and high vibration levels when the vehicle passes over it with speeds higher than the allowable speed limit. If this shock is strong enough, it can cause severe spinal injuries [16]. Good response to a pothole input is a good indication that a control scheme will provide good performance for other excitations.

3.5. Passive Suspension Design

In the design of a passive suspension to find suitable damping and stiffness constants is important. The matrices D_{12} and D_{22} turn out to be zero in the passive suspension case. Consider the system defined below

$$\begin{aligned} \dot{\tilde{x}} &= \begin{bmatrix} A & B_1 C_w \\ 0 & A_w \end{bmatrix} \tilde{x} + \begin{bmatrix} 0 \\ B_w \end{bmatrix} v \\ z &= \begin{bmatrix} C_1 & D_{11} C_w \end{bmatrix} \tilde{x} \end{aligned} \tag{3.47}$$

Equation (3.47) defines the passive system. It is the same as (3.45), but active forces and measured output vector y are ignored.

3.5.1. Optimal spring and damping constants

In designing passive suspension it is important to use realistic parameter values. The nominal vehicle parameters selected for this study are shown in Table 3.3. In this section frequency response of the passive model is illustrated under different damping parameters.

Table 3.3. Parameters used for the passively suspended half-car model

Symbols	Units	Values
K_f	N/m	22000
K_r	N/m	22000
K_t	N/m	160000
M_s	kg	500
J	kg. m^2	2700
m_{uf}	kg	50
m_{ur}	kg	50
l_f	m	1.5
l_r	m	2.5
l_d	m	0.3

In order to find the suitable damping values for the design, frequency responses of the outputs are plotted for the three different damping values as shown in figure 3.4. Front wheel road disturbances are considered for the all responses. Passive system natural frequencies occur at around 1.59 and 9.54 Hz thus between 10 rad/s and 60 rad/s. It is important to consider the frequency level of the outputs between the natural frequencies and the peak values at those points.

Vertical acceleration response curves are shown in figure 3.4.a. For a large damping, (Cs=3920 Dash-dot) there are no resonances at the sprung mass and the wheelhop modes. For the low damping (Cs=196 Dashed), there is a significant increase around the sprung mass natural frequency. Considering this the reasonable damping value is chosen as 980 Ns/m. The effect of the suspension damping on vertical acceleration and suspension deflection are detailed in reference [6].

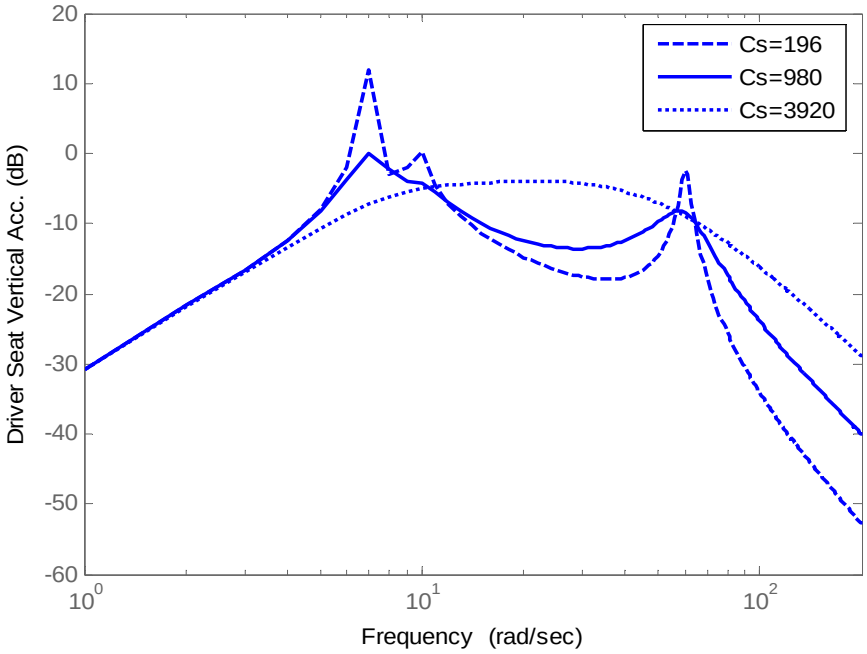

(a)

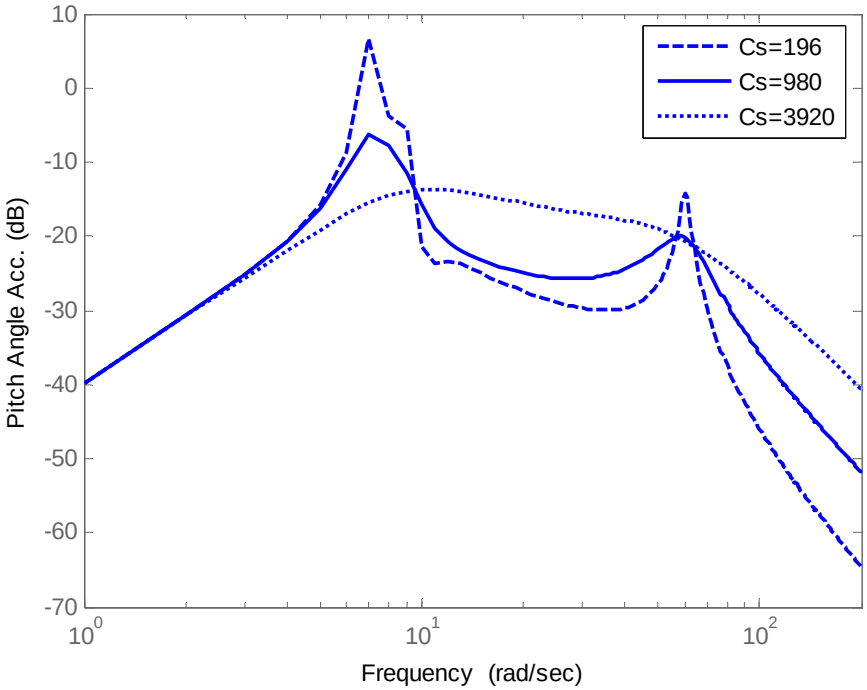

(b)

Figure 3.4. Effect of damping on the response of the passive suspension

Cs=980 (Solid), Cs=196 (Dashed), Cs=3920, (dot)

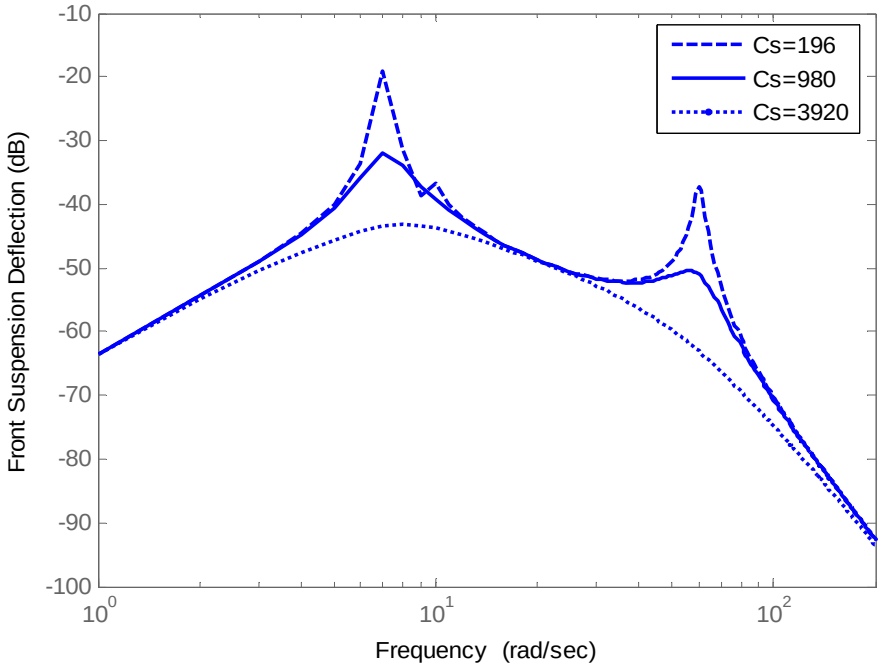

(c)

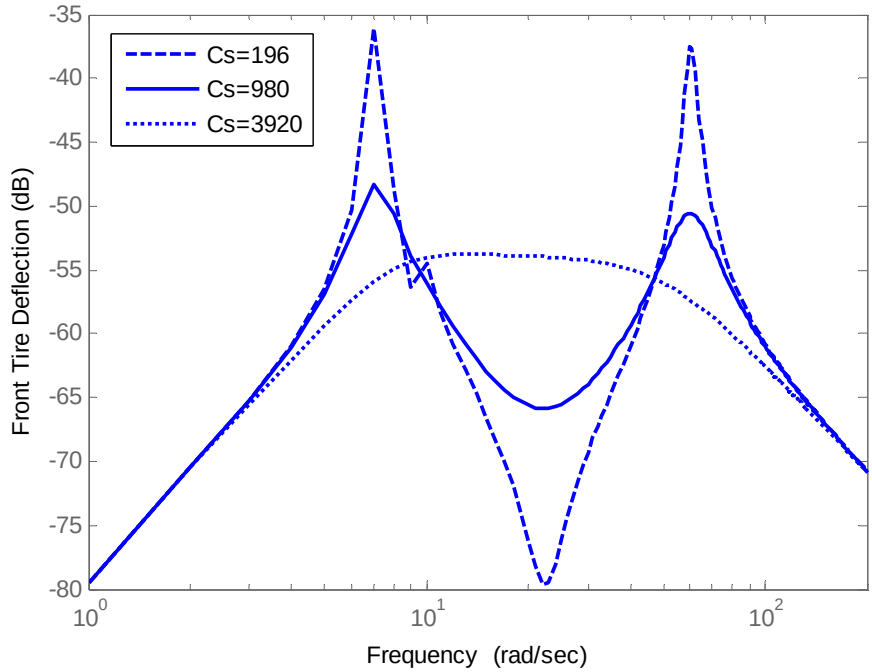

(d)

Figure 3.4. (Continued) Effect of damping on the response of a passive suspension

Cs=980 (Solid), Cs=196 (Dashed), Cs=3920, (dot)

4. LQG REGULATOR DESIGN

In the LQG framework, the *separation principle* applies. By the separation principle, the solution to the LQG problem consists of an optimal state estimator and an optimal state feedback controller that are designed independently. The name LQG is used because the problem involves a linear system, a quadratic cost function and Gaussian white process and measurement noise.

Equation (4.1) below is the same as (3.45) and shows the state space formulation of the system with the regulated outputs considering colored noise inputs as disturbances.

$$\begin{aligned} \dot{\widetilde{x}} &= \widetilde{A}\widetilde{x} + \widetilde{B}_1 v + \widetilde{B}_2 u \\ \widetilde{z} &= \widetilde{C}_1 \widetilde{x} + D_{12} u \\ \widetilde{y} &= \widetilde{C}_2 \widetilde{x} + D_{22} u \end{aligned} \tag{4.1}$$

The performance index, J is typically formulated in the standard LQ manner to minimize the outputs. Since the system has a disturbance state it is convenient to choose the optimal control to minimize the cost function described by

$$\begin{aligned} J = \int_0^\infty \{ & \lambda_1 [\ddot{z}_d(t)]^2 + \lambda_2 [\ddot{\theta}(t)]^2 + \\ & \lambda_3 [z_{sf}(t) - z_{uf}(t)]^2 + \lambda_3 [z_{sr}(t) - z_{ur}(t)]^2 + \\ & \lambda_4 [z_{uf}(t) - z_{fr}(t)]^2 + \lambda_4 [z_{ur}(t) - z_{rr}(t)]^2 + \\ & \lambda_5 [u_1(t)]^2 + \lambda_5 [u_2(t)]^2 \} dt \end{aligned} \tag{4.2}$$

Here, the cost function for the LQG formulation is chosen to weigh the driver seat vertical acceleration, pitch angle acceleration, suspension and tire deflections, for the front and rear sides.

The values of the weighting coefficients $\lambda_1 - \lambda_5$ are chosen according to the importance placed on each performance measure. Large gains λ_1, λ_2 and small gains λ_3, λ_4 correspond to a design that emphasizes passenger comfort. This cost function is then placed in the standard form:

$$J = \int_0^\infty [\tilde{x}^T Q x + u^T R u + 2\tilde{x}^T N u] dt \tag{4.3}$$

where the matrices Q, R and N are design parameters which will be obtained in the following sections.

4.1. Optimal State Feedback Controller Design

In this study the optimal state feedback controller is taken as linear quadratic regulator (LQR). This formulation is chosen because the aim is to regulate the deviation of the vehicle (regulated outputs) from its equilibrium state.

The linear quadratic Gaussian (LQG) problem is to find the control input $u(t)$ that minimizes the quadratic performance index J in (4.3). Actually, LQG is the combination of the LQR with an observer which is detailed in the following section.

The optimal controller is a feedback controller K_c operating on $\tilde{x}$, and the optimal control law is given by

$$u(t) = K_c \tilde{x}(t) \tag{4.4}$$

where

$$K_c = -R^{-1} B_2{}^T P \tag{4.5}$$

and P is determined by solving the Algebraic Riccatti Equation (ARE):

$$A^T P + PA - (PB + N) R^{-1} (B^T P + N^T) + Q = 0 \tag{4.6}$$

Here, K is a m × n matrix where m is the number of the control inputs and n is the number of the state variables. For the eighth order system with two second order colored noise inputs, the resulting gain matrix is of size 2 × 12, with the first row corresponding to the front actuator, and the second row corresponding to the rear actuator. The gain matrix K_c is computed by lqr command in MATLAB. The design parameters Q, R and N are computed as follows.

First RMS values of the outputs are defined as:

$$\ddot{z}_d = a_1\tilde{x} + b_1 u$$

$$\ddot{z}_d{}^2 = (a_1\tilde{x} + b_1 u)^T (a_1\tilde{x} + b_1 u)$$

$$= \begin{bmatrix} \tilde{x} \\ u \end{bmatrix}^T \begin{bmatrix} a_1 & b_1 \end{bmatrix}^T \begin{bmatrix} a_1 & b_1 \end{bmatrix} \begin{bmatrix} \tilde{x} \\ u \end{bmatrix} \tag{4.7}$$

$$\ddot{\theta} = a_2\tilde{x} + b_2 u$$

$$\ddot{\theta}^2 = (a_2\tilde{x} + b_2 u)^T (a_2\tilde{x} + b_2 u)$$

$$= \begin{bmatrix} \tilde{x} \\ u \end{bmatrix}^T \begin{bmatrix} a_2 & b_2 \end{bmatrix}^T \begin{bmatrix} a_2 & b_2 \end{bmatrix} \begin{bmatrix} \tilde{x} \\ u \end{bmatrix} \tag{4.8}$$

Let $e_n{}^T$ denote the unit vectors in IR^j and where $j = \dim(\tilde{x}) + \dim(u)$

$$(z_{sf} - z_{uf}) = (e_1 + l_d e_2 - e_3) \begin{bmatrix} \tilde{x} \\ u \end{bmatrix}$$

$$(z_{sf} - z_{uf})^2 = \begin{bmatrix} \tilde{x} \\ u \end{bmatrix}^T (e_1 + l_d e_2 - e_3)^T (e_1 + l_d e_2 - e_3) \begin{bmatrix} \tilde{x} \\ u \end{bmatrix} \tag{4.9}$$

$$(z_{sr} - z_{ur})^2 = \begin{bmatrix} \tilde{x} \\ u \end{bmatrix}^T (e_1 - l_d e_2 - e_4)^T (e_1 - l_d e_2 - e_4) \begin{bmatrix} \tilde{x} \\ u \end{bmatrix} \tag{4.10}$$

From section 3.4.1,

$$C_w = \begin{bmatrix} 0 & 0.1809 \end{bmatrix} \text{ and } w(t) = C_w x_v(t)$$

$$(z_{uf} - z_{fr})^2 = \begin{bmatrix} \tilde{x} \\ u \end{bmatrix}^T (e_3 - 0.1809 e_{10})^T (e_3 - 0.1809 e_{10}) \begin{bmatrix} \tilde{x} \\ u \end{bmatrix} \tag{4.11}$$

$$(z_{ur} - z_{rr})^2 = \begin{bmatrix} \tilde{x} \\ u \end{bmatrix}^T (e_4 - 0.189 e_{12})^T (e_4 - 0.1809 e_{12}) \begin{bmatrix} \tilde{x} \\ u \end{bmatrix} \tag{4.12}$$

The actuator effort must also be included in the cost function to ensure that it remains bounded. Thus,

$$u_1^{\,2} = \begin{bmatrix} \tilde{x} \\ u \end{bmatrix}^T (e_{n+1}^T e_{n+1}) \begin{bmatrix} \tilde{x} \\ u \end{bmatrix} \tag{4.13}$$

$$u_2^{\,2} = \begin{bmatrix} \tilde{x} \\ u \end{bmatrix}^T (e_{n+2}^T e_{n+2}) \begin{bmatrix} \tilde{x} \\ u \end{bmatrix} \tag{4.14}$$

and by using (4.7) through (4.14) in (4.2) the cost function J is rewritten as:

$$\begin{aligned} J(u) = \int_0^\infty \begin{bmatrix} \tilde{x} \\ u \end{bmatrix}^T \{ & \lambda_1 \begin{bmatrix} a_1 & b_1 \end{bmatrix}^T . \begin{bmatrix} a_1 & b_1 \end{bmatrix} + \lambda_2 \begin{bmatrix} a_2 & b_2 \end{bmatrix}^T . \begin{bmatrix} a_2 & b_2 \end{bmatrix} \\ & + \lambda_3 (e_1 + l_d e_2 - e_3)^T (e_1 + l_d e_2 - e_3) \\ & + \lambda_3 (e_1 - l_d e_2 - e_4)^T (e_1 - l_d e_2 - e_4) \\ & + \lambda_4 (e_3 - 0.1809)^T (e_3 - 0.1809) \\ & + \lambda_4 (e_4 - 0.1809)^T (e_4 - 0.1809) \\ & + \lambda_5 (e_{n+1}^T e_{n+1}) + \lambda_5 (e_{n+2}^T e_{n+2})] \} . \begin{bmatrix} \tilde{x} \\ u \end{bmatrix} dt \end{aligned} \tag{4.15}$$

The cost function J is then placed in the standard form:

$$J = \int_0^\infty \begin{bmatrix} \tilde{x} \\ u \end{bmatrix}^T \begin{bmatrix} Q & N \\ N^T & R \end{bmatrix} \cdot \begin{bmatrix} \tilde{x} \\ u \end{bmatrix} dt \tag{4.16}$$

or more compactly,

$$J = \int_0^\infty \begin{bmatrix} \tilde{x} \\ u \end{bmatrix}^T Q_\pi \begin{bmatrix} \tilde{x} \\ u \end{bmatrix} dt \tag{4.17}$$

where Q_π is the quadratic performance index,

$$Q_\pi = \begin{bmatrix} Q & N \\ N^T & R \end{bmatrix} \tag{4.18}$$

As stated at the end of the section 3.3, (3.38) represents the state-space formulation of the half-car vehicle system without a reference to a disturbance model included to the system. The optimal state feedback controller configuration for this system is shown in figure 4.1

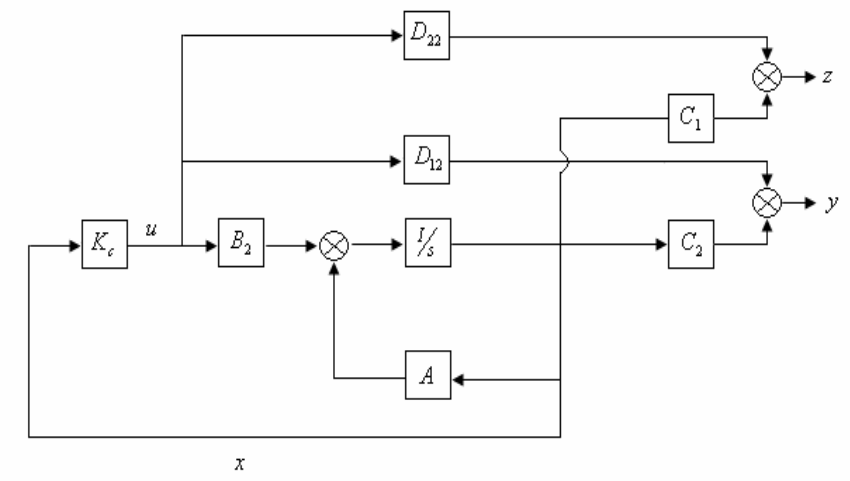

Figure 4.1. Linear quadratic regulator

Equation (3.44) describes the combined vehicle model and the road model. (3.44) can be combined with the optimal state feedback controller and the corresponding block diagram of the overall system is shown in figure 4.2

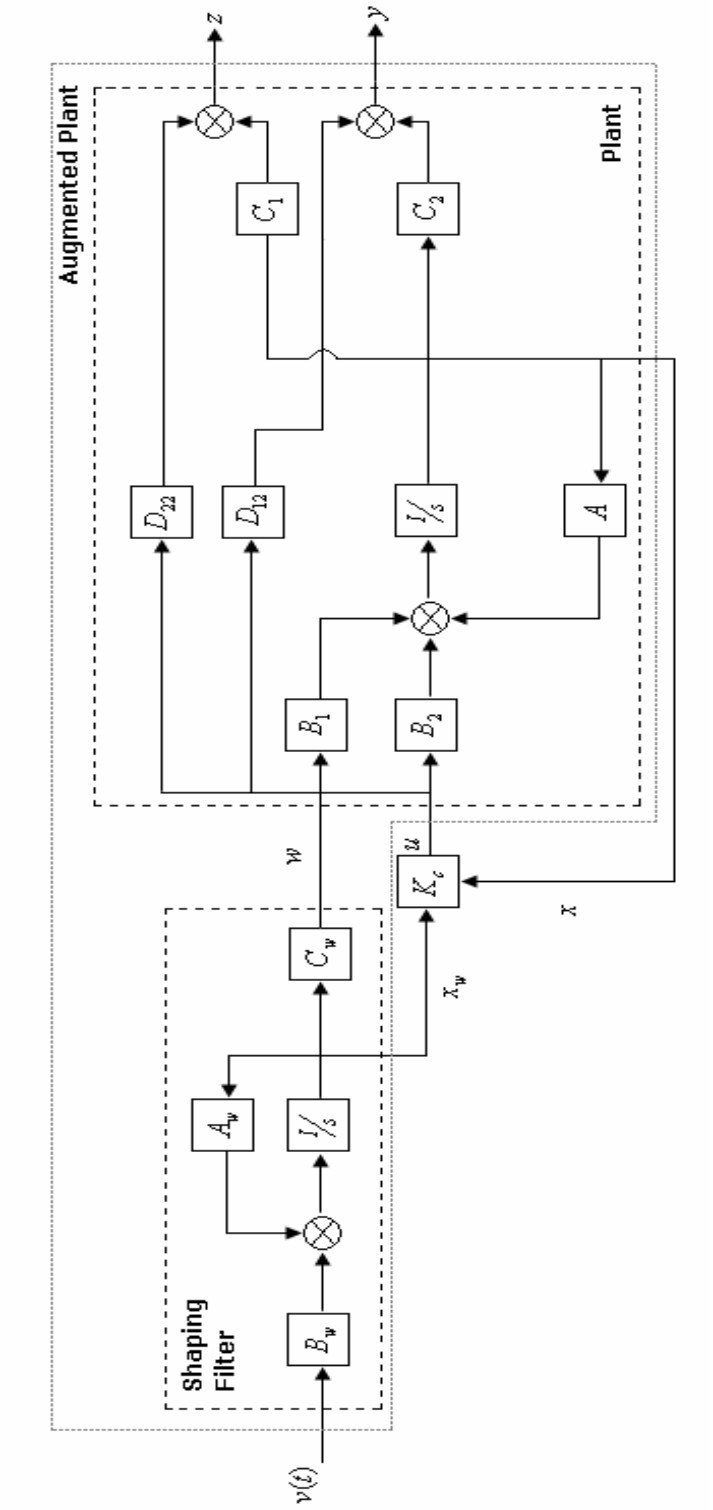

Figure 4.2. Detailed model showing the shaping filter and the plant

Simplified form of (3.44) was written as (3.45) and corresponding block diagram is shown in figure 4.3

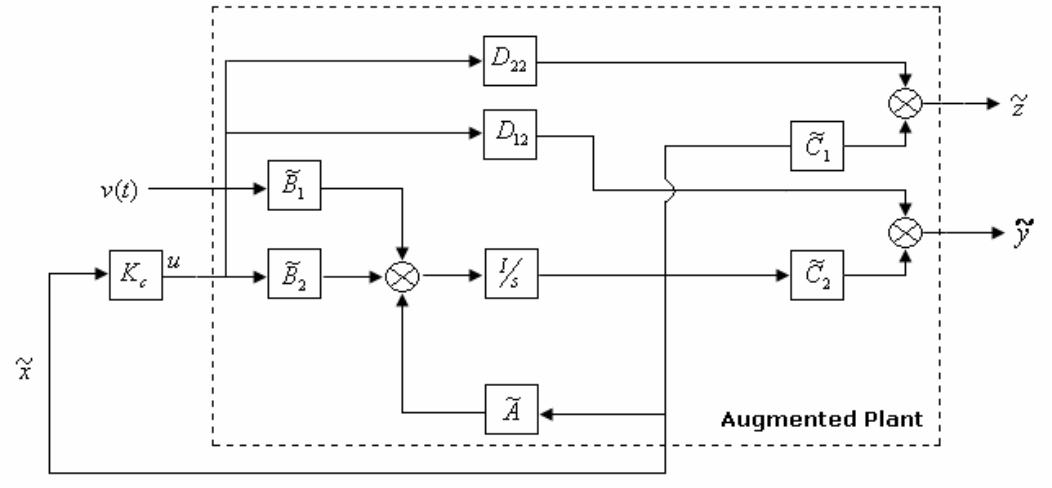

Figure 4.3. Simplified model showing the augmented plant

4.2. Optimal State Estimator Design

Due to practical limitations, all the states required for the state-feedback controller are not measurable, thus an observer is used to observe the states. Otherwise a large number of sensors must be used. In the LQG design presented in this study it is assumed that not all the internal states of the system and all the disturbance states are available for feedback which is true for the most cases. Therefore Kalman state observer is designed. It is also known that while the number of sensors used increases the cost, the use of a state estimator lowers the performance of the control system.

For the estimator design consider the following system model:

$$\begin{aligned} \dot{\tilde{x}} &= \tilde{A}\tilde{x} + \tilde{B}_1 v + \tilde{B}_2 u \\ \tilde{z} &= \tilde{C}_1 \tilde{x} + D_{12} u \\ \tilde{y} &= \tilde{C}_2 \tilde{x} + D_{22} u + \theta \end{aligned} \tag{4.19}$$

In (4.19), an artificial sensor noise θ is introduced. Then covariance structure is defined as follows:

$$\begin{aligned} Q &= E\{vv^T\} = 1, \\ R &= E\{\theta\theta^T\} = 0{,}001, \\ N &= E\{\theta v^T\} = E\{v\theta^T\} = 0 \end{aligned} \tag{4.20}$$

where $E\{.\}$ is the mean value operator and Q, R and N are the matrices mentioned in (4.3). Then, for the estimation procedure it can proceed as follows.

The optimal state estimator is a Kalman filter. The state estimator uses noisy measurements $\tilde{y}$ and the control input u to generate estimates $\hat{x}$ of $\tilde{x}$.

Kalman filter state is

$$\dot{\hat{x}} = \tilde{A}\hat{x} + \tilde{B}_2 u + K_f(\tilde{y} - \tilde{C}_2\hat{x} - D_{22}u) \tag{4.21}$$

and the problem is to find K_f to minimize the estimation error

$$E\{(\tilde{x} - \hat{x})^T(\tilde{x} - \hat{x})\}. \tag{4.22}$$

The optimal choice of K_f can be evaluated from

$$K_f = P\tilde{C}_2^{\,T} R^{-1} \tag{4.23}$$

Where P is the positive definite solution of the Ricatti equation,

$$AP + PA^T - PC^T R^{-1} CP + Q = 0 \tag{4.24}$$

As a note, in (4.5) $\hat{x}$ is a function of output $\tilde{y}$

$$\tilde{y} = \tilde{C}_2\tilde{x} + D_{22}u \tag{4.25}$$

but the input u itself is generated by a state feedback law as

$$u = -K_c\hat{x} \tag{4.26}$$

Thus, for simulation purpose the system dynamics (4.25) can be augmented with that of the observer equation (4.21). First by plugging (4.26) into (4.21) and (4.25) to obtain:

$$\dot{\hat{x}} = (\widetilde{A} + D_{22}K_c - \widetilde{B}_2K_c - K_f\widetilde{C}_2)\hat{x} + K_f\widetilde{y} \tag{4.27}$$

$$\widetilde{y} = \widetilde{C}_2\widetilde{x} - D_{22}K_c\hat{x} \tag{4.28}$$

and resulting Kalman estimator can be formed by plugging (4.28) into (4.27)

$$\dot{\hat{x}} = (\widetilde{A} - \widetilde{B}_2K_c - K_f\widetilde{C}_2)\hat{x} + K_f\widetilde{C}_2\widetilde{x} \tag{4.29}$$

then Kalman state combines with the system by plugging (4.26) into (4.1)

$$\begin{aligned} \dot{\widetilde{x}} &= \widetilde{A}x + \widetilde{B}_1\nu - \widetilde{B}_2K_c\hat{x} \\ \widetilde{z} &= \widetilde{C}_1\widetilde{x} - K_cD_{12}\hat{x} \end{aligned} \tag{4.30}$$

Now state feedback and the state estimator are designed. The gain matrix K_f is computed by lqe command in MATLAB. Finally a new state vector can be written by forming an augmented state vector $\bar{x}$:

$$\bar{x} = \begin{bmatrix} \widetilde{x} \\ \hat{x} \end{bmatrix}, \text{ closed loop state vector} \tag{4.31}$$

including the system states $\widetilde{x}$ and the disturbance state $\hat{x}$. And then, closed-loop dynamics of the system can be described by using augmented state vector $\bar{x}$:

$$\dot{\bar{x}} = \begin{bmatrix} \widetilde{A} & -\widetilde{B}_2K_c \\ K_f\widetilde{C}_2 & \widetilde{A} - \widetilde{B}_2K_c - K_f\widetilde{C}_2 \end{bmatrix}\bar{x} + \begin{bmatrix} \widetilde{B}_1 \\ 0 \end{bmatrix}\nu$$

$$\bar{z} = \begin{bmatrix} \widetilde{C}_1 & -D_{12}K_c \end{bmatrix}\dot{\bar{x}} \tag{4.32}$$

or more compactly

$$\begin{aligned} \dot{\bar{x}} &= A_c\bar{x} + B_c\nu \\ \bar{z} &= C_c\bar{x} \end{aligned} \tag{4.33}$$

The optimal state feedback controller and the optimal state estimator may be combined as shown in figure 4.4 to form an LQG controller. This controller uses a set of noisy output measurements, control signal measurements and an internal model of the system dynamics to provide optimal regulation of the plant [12].

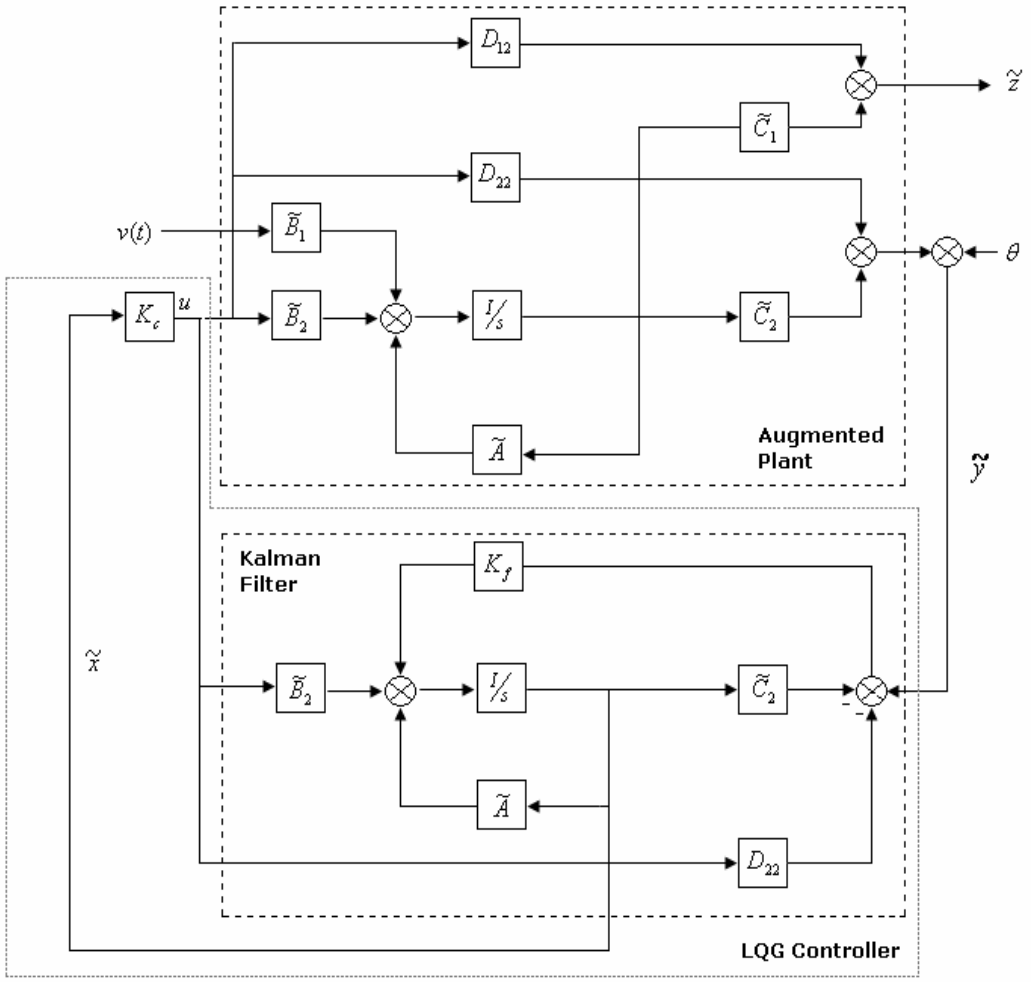

Figure 4.4. Linear quadratic Gaussian controller

Heave and pitch acceleration of the sprung mass with suspension and tire deflections are taken as input data of the LQG controller. Actuator forces improving vehicle driving, ride comfort and handling properties are considered to be the controller outputs.

4.3. Determining Weighting Coefficients

The problem of controller design is a challenge for finding suitable weightings that satisfies the design performances. In order to find appropriate weights stochastic inputs are applied to simulate realistic road surface conditions. In this way trade-off curves which are used to find parameters that constitute the performance index are obtained. Now, recall (4.17) which is rewritten below.

$$J = \int_0^\infty \begin{bmatrix} \tilde{x} \\ u \end{bmatrix}^T Q_\pi \begin{bmatrix} \tilde{x} \\ u \end{bmatrix} dt \tag{4.34}$$

Minimizing procedure of J starts by finding Q_π . Before to find Q_π the coefficients $\lambda_1 - \lambda_5$ are found. These coefficients are mentioned in (4.2) and (4.15).

As stated in the section 3.4 while it is not possible to predict the value of the ride input at any specific instant of time it is possible to describe stochastic ride inputs by filtering white noise. Nondeterministic inputs are applied to simulate the road surface conditions more realistically. With these inputs, stochastic response of the system which will enable us to weight outputs of the system by selecting proper $\lambda's$ is obtained.

Now, consider the system defined by (3.38),

$$\begin{aligned} \dot{x} &= Ax + B_1 w + B_2 u \\ z &= C_1 x + D_{11} w + D_{12} u \\ y &= C_2 x + D_{21} w + D_{22} u \end{aligned} \tag{4.35}$$

When stochastic response of the system is considered, delay between rear and front wheels must be included in the model.

The disturbance, z_{r2} at the rear wheel is identical to the disturbance, z_{r1} at the front wheel except for a pure time delay. Note that z_{r1} and z_{r2} are uncorrelated for the time delay between them

$$z_{r2} = z_{r1} \exp(-l/v) \tag{4.36}$$

or

$$w_2(t) = w_1(t-\tau) \tag{4.37}$$

where l is the distance between front and rear wheels,

$$\tau = \frac{l_f + l_r}{v} \tag{4.38}$$

and τ is the time delay between the two wheels. Approximating delay τ Pade expansion of degree three

$$\begin{aligned} \dot{x}_p &= A_p x_p + B_p w_1 \\ w_2 &= c_p x_p + d_p w_1 \end{aligned} \tag{4.39}$$

is used and then by using state-space formulation of Pade expansion defined in (4.39), road input vector is written as:

$$w = \begin{bmatrix} w_1 \\ w_2 \end{bmatrix} = \begin{bmatrix} 0_{1x3} \\ c_p \end{bmatrix} x_p + \begin{bmatrix} 1 \\ d_p \end{bmatrix} w_1 \tag{4.40}$$

or more compactly

$$w = C_p x_p + D_p w_1 \tag{4.41}$$

and plugging (4.41) into (3.38) the system dynamics are

$$\begin{aligned} \dot{x} &= Ax + B_1(C_p x_p + D_p w_1) + B_2 u \\ z &= C_1 x + D_{11}(C_p x_p + D_p w_1) + D_{12} u \\ y &= C_2 x + D_{21}(C_p x_p + D_p w_1) + D_{22} u \end{aligned} \tag{4.42}$$

State-space formulation of the system can be rewritten by forming an augmented state vector:

$$\hat{x} = \begin{bmatrix} x \\ x_p \end{bmatrix} \tag{4.43}$$

Including the system states x and state of the Pade system x_p. The augmented state-space model of the system is described by

$$\begin{aligned} \dot{\hat{x}} &= \begin{bmatrix} A & B_1 C_p \\ 0 & A_p \end{bmatrix} \hat{x} + \begin{bmatrix} B_1 D_p \\ B_p \end{bmatrix} w_1 + \begin{bmatrix} B_2 \\ 0 \end{bmatrix} u \\ z &= \begin{bmatrix} C_1 & D_{11} C_p \end{bmatrix} \hat{x} + D_{11} D_p w_1 + D_{12} u \\ y &= \begin{bmatrix} C_2 & D_{21} C_p \end{bmatrix} \hat{x} + D_{21} D_p w_1 + D_{22} u \end{aligned} \tag{4.44}$$

or more compactly

$$\begin{aligned} \dot{\hat{x}} &= \hat{A}\hat{x} + \hat{B}_1 w_1 + \hat{B}_2 u \\ z &= \hat{C}_1 \hat{x} + \hat{D}_{11} w_1 + \hat{D}_{12} u \\ y &= \hat{C}_2 \hat{x} + \hat{D}_{21} w_1 + \hat{D}_{22} u \end{aligned} \tag{4.45}$$

System dynamics can be rewritten by using the state

$$\tilde{x} = \begin{bmatrix} \dot{\hat{x}} \\ \dot{x}_v \end{bmatrix} \tag{4.46}$$

Then augmented representation of the system is

$$\begin{aligned} \dot{\tilde{x}} &= \begin{bmatrix} \hat{A} & B_1 C_v \\ 0 & A_v \end{bmatrix} \tilde{x} + \begin{bmatrix} 0 \\ B_v \end{bmatrix} v + \begin{bmatrix} \hat{B}_2 \\ 0 \end{bmatrix} u \\ z &= \begin{bmatrix} \hat{C}_1 & \hat{D}_{11} C_v \end{bmatrix} \tilde{x} + \hat{D}_{12} u \\ y &= \begin{bmatrix} \hat{C}_2 & \hat{D}_{21} C_v \end{bmatrix} \tilde{x} + \hat{D}_{22} u \end{aligned} \tag{4.47}$$

or simply

$$\begin{aligned}\dot{\tilde{x}} &= \tilde{A}\tilde{x} + \tilde{B}_1 v + \tilde{B}_2 u \\ z &= \tilde{C}_1 \tilde{x} + D_{12} u \\ y &= \tilde{C}_2 \tilde{x} + D_{22} u\end{aligned} \tag{4.48}$$

Equation (4.48) is identical with (4.1) but time delay between the two wheels is defined in this case. Then state feedback and state estimator are designed for the system in the same manner as in explained in the sections 4.1 and 4.2. After feedback and observer gains, K_c and K_f are obtained closed loop design is completed. These procedures are not explained again and closed loop configuration of the system is written below.

$$\begin{aligned}\dot{\bar{x}} &= \begin{bmatrix} \tilde{A} & -\tilde{B}_2 K_c \\ K_f \tilde{C}_2 & \tilde{A} - \tilde{B}_2 K_c - K_f \tilde{C}_2 \end{bmatrix} \bar{x} + \begin{bmatrix} \tilde{B}_1 \\ 0 \end{bmatrix} v \\ \bar{x} &= \begin{bmatrix} \tilde{C}_1 & -D_{12} K_c \end{bmatrix} \dot{\bar{x}}\end{aligned} \tag{4.49}$$

or simply

$$\begin{aligned}\dot{\bar{x}} &= A_c \bar{x} + B_c v \\ \bar{z} &= C_c \bar{x}\end{aligned} \tag{4.50}$$

Equation (4.50) represents closed loop configuration of the system. By using (4.50) RMS and frequency response of the system are obtained and for the RMS response the state covariance matrix P_x can be calculated by solving the Lyapunov equation,

$$A_c P_x + P_x A_c + BB^T = 0 \tag{4.51}$$

By lyap command in MATLAB and then output covariance matrix P_y is

$$P_y = C_{cl} P_x {C_{cl}}^T \tag{4.52}$$

Square root of P_y is RMS response of the system. Figures 4.5 and 4.6 show trade-off curves.

4.3.1. Trade-off curves

In order to observe the trade-offs between regulated outputs of the system, first λ_2 and λ_3 which weight pitch acceleration and suspension-tire deflections are fixed at 150 and 1, respectively, and the value of λ_1 is varied over the range from 1 to 500. Weights for the actuators are set to be 3.10^{-4}. Trade-off curve to weight heave acceleration is shown in figure 4.5.a. In these plots one can see that the optimum value for λ_1 is 150. For the λ_1 above 150, rms value of the driver seat vertical acceleration decreases but rms pitch acceleration, suspension and tire deflections increase. Therefore it is not convenient to increase λ_1 further more.

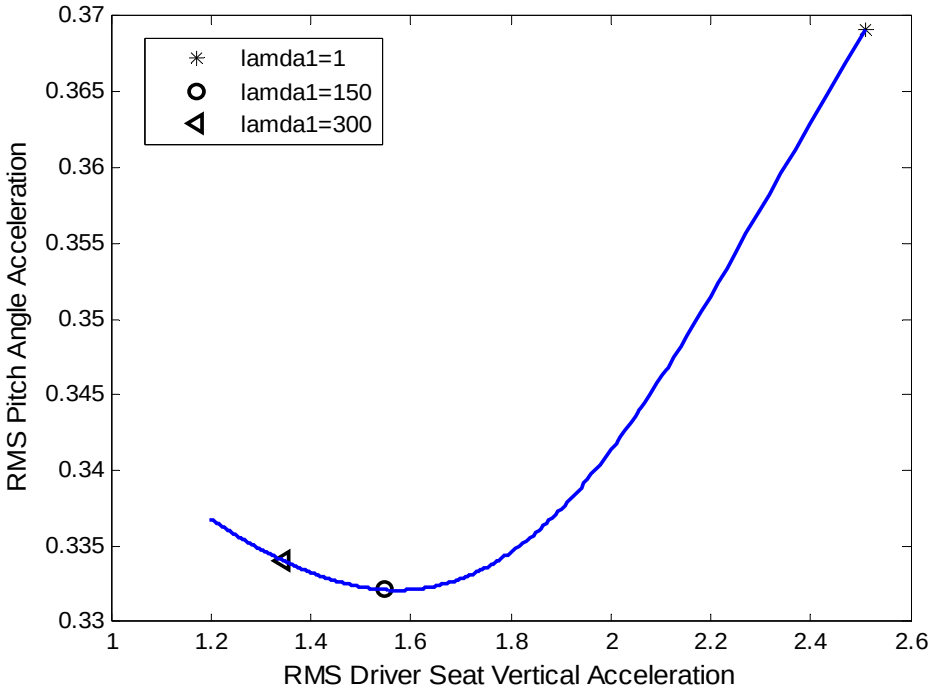

(a)

Figure 4.5. Trade-off curves to weight driver seat vertical acceleration

($1 < \lambda_1 < 500$, $\lambda_2 = 150$, $\lambda_3 = \lambda_4 = 1$, $\lambda_4 = \lambda_5 = 0{,}0003$ @ v=108 km/h)

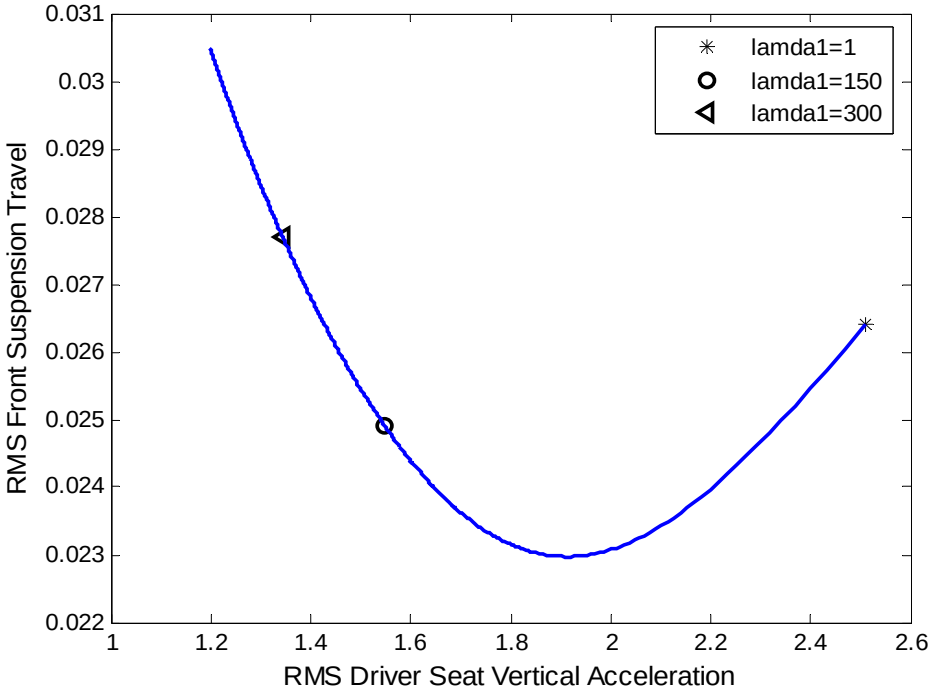

(b)

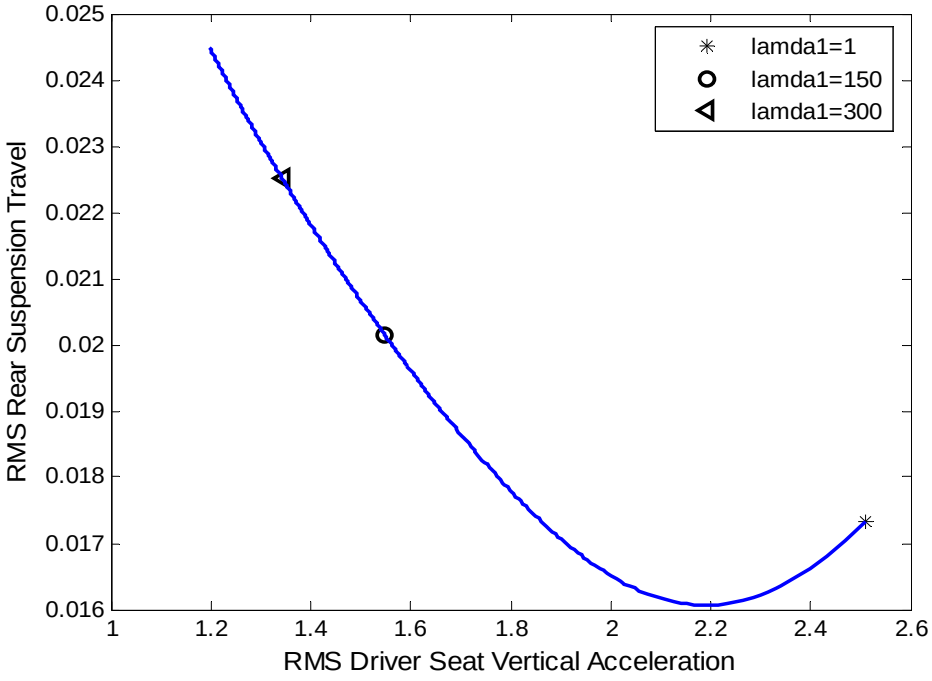

(c)

Figure 4.5. (Continued) Trade-off curves to weight driver seat vertical acceleration

($1 < \lambda_1 < 500, \lambda_2 = 150, \lambda_3 = \lambda_4 = 1, \lambda_4 = \lambda_5 = 0{,}0003$ @ v=108 km/h)

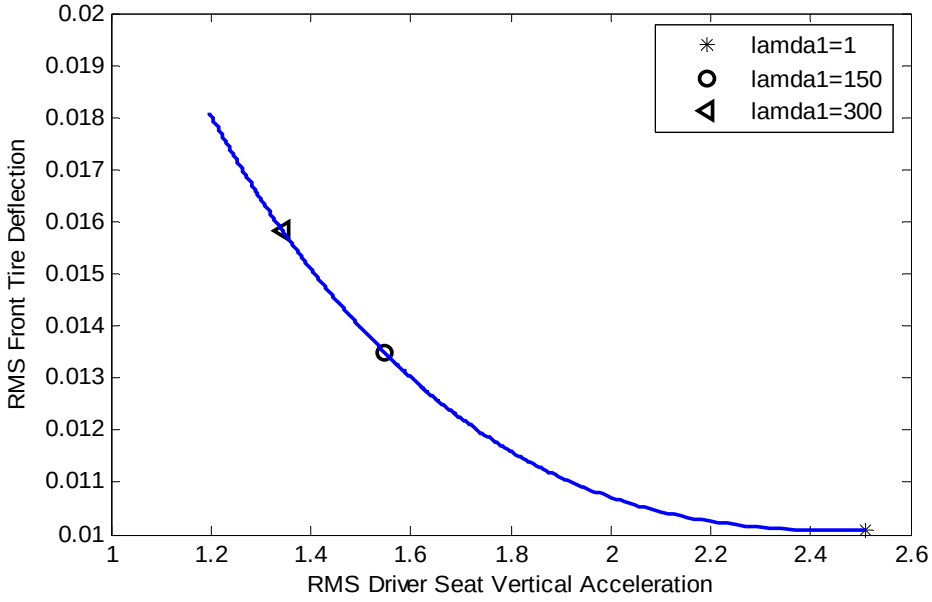

(d)

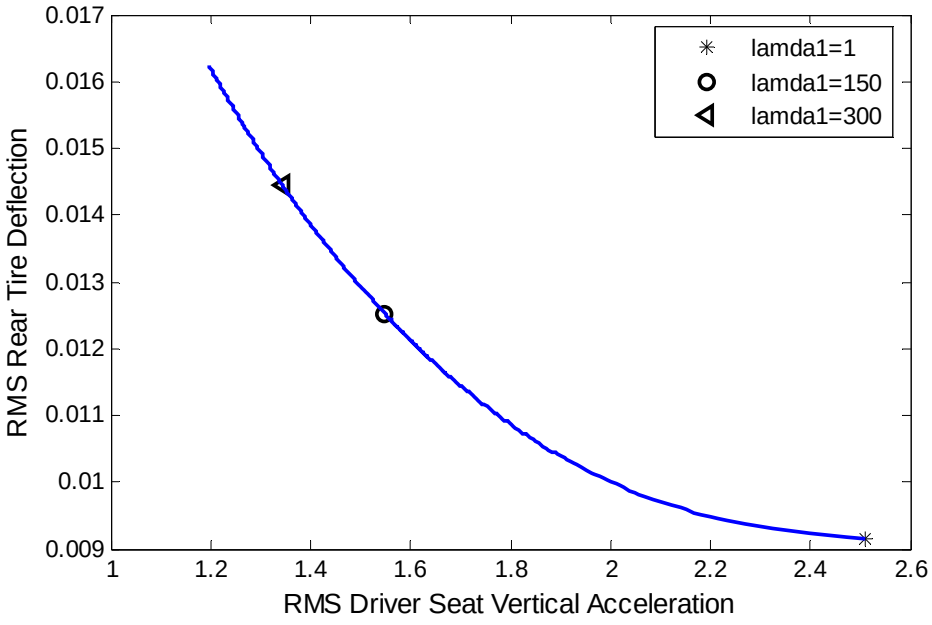

(e)

Figure 4.5. (Continued) Trade-off curves to weight driver seat vertical acceleration

$(1 < \lambda_1 < 500, \lambda_2 = 150, \lambda_3 = \lambda_4 = 1, \lambda_4 = \lambda_5 = 0{,}0003$ @ v=108 km/h)

In order to obtain optimum value for λ_2 the same procedure applies. But in this case λ_1 is set to be 150 and the value of λ_2 is varied over the range from 1 to 500. Analyzing figure 4.6 one notices that the optimum value for λ_2 is 150. As a note, for the outputs, greater weight means more decrease and smaller weight correspond more increase in rms. Trade-off curves to weight pitch acceleration is shown in figure 4.6.a. In this case, as the λ_2 increased, pitch and heave acceleration have a small decrease, but front suspension and tire deflections increases. Thus λ_2 is set to be 150.

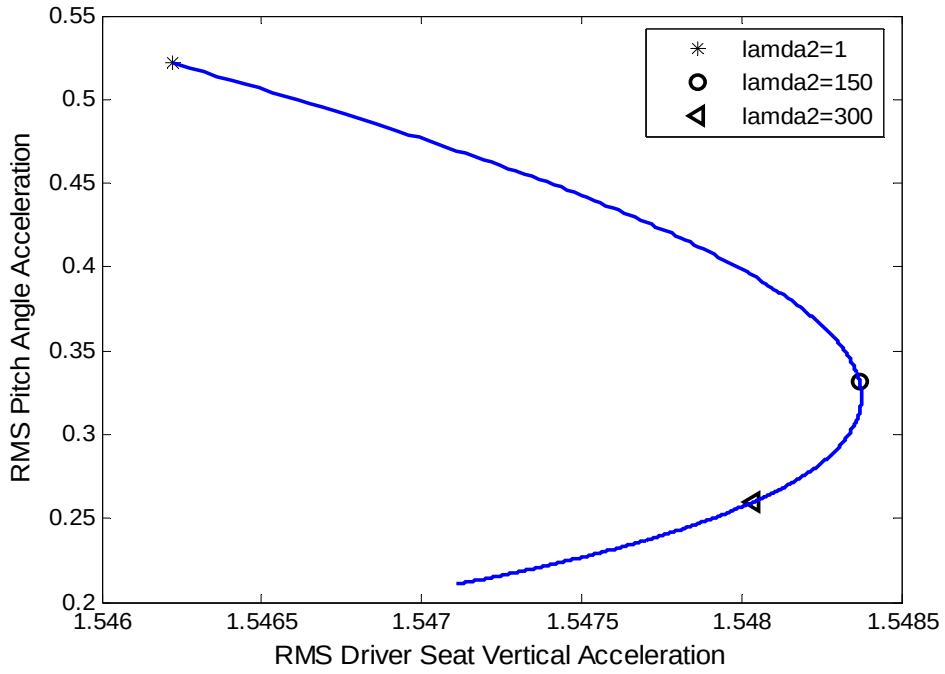

(a)

Figure 4.6. Trade-off curves to weight pitch angle acceleration

($\lambda_1 = 150, 1 < \lambda_2 < 500, \lambda_3 = \lambda_4 = 1, \lambda_4 = \lambda_5 = 0{,}0003$ @ v=108 km/h)

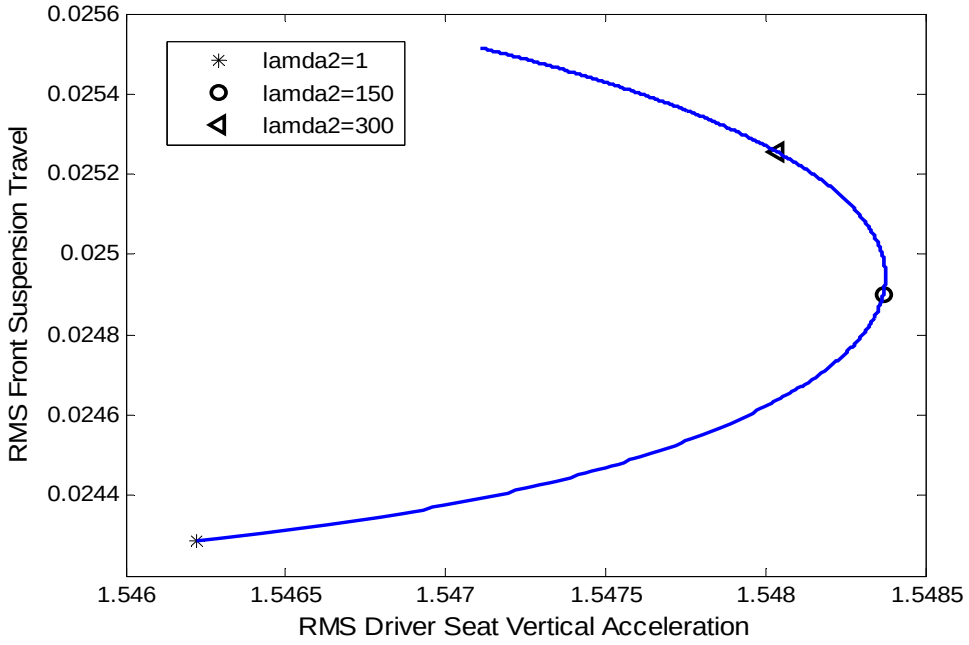

(b)

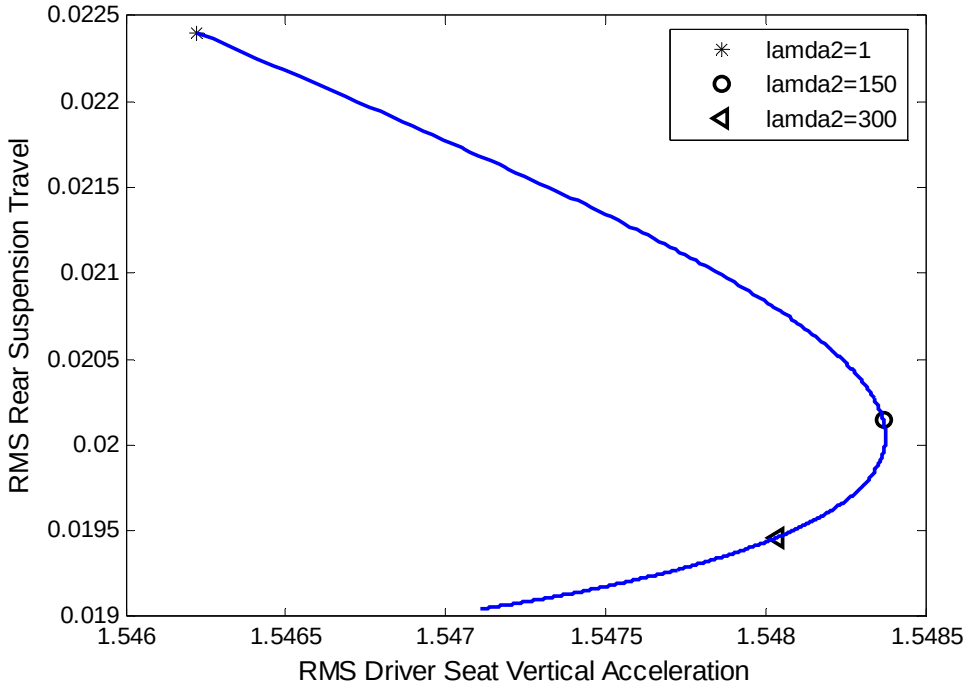

(c)

Figure 4.6. **(Continued)** Trade-off curves to weight pitch angle acceleration

($\lambda_1 = 150, 1 < \lambda_2 < 500, \lambda_3 = \lambda_4 = 1, \lambda_4 = \lambda_5 = 0{,}0003$ @ v=108 km/h)

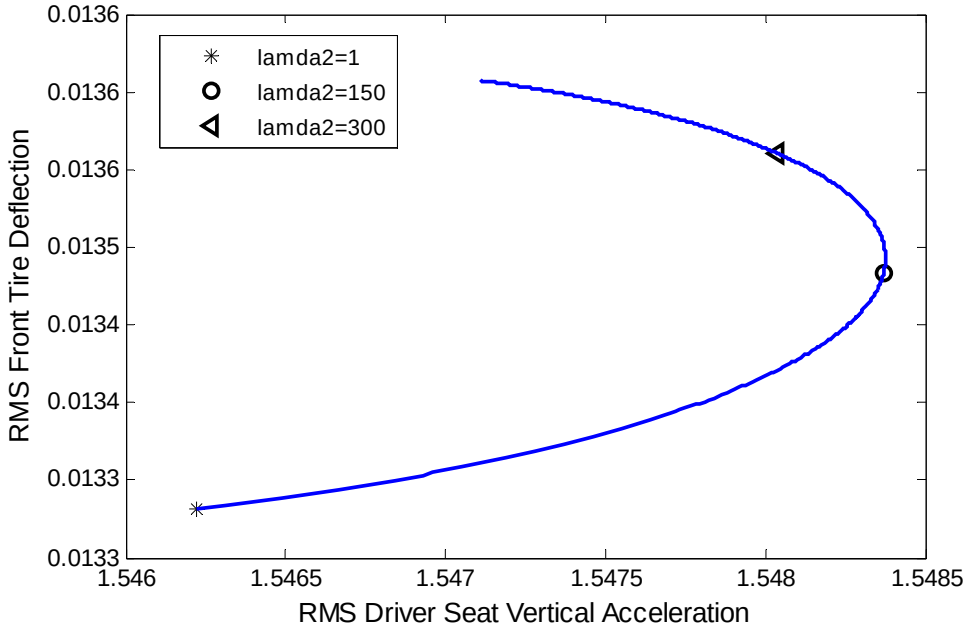

(d)

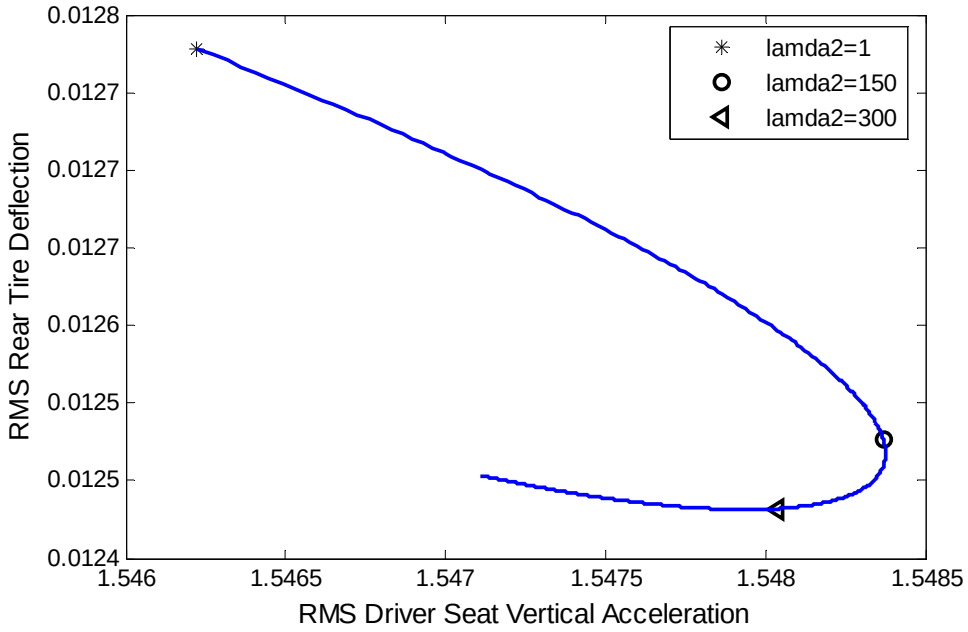

(e)

Figure 4.6. (Continued) Trade-off curves to weight pitch angle acceleration

($\lambda_1 = 150{,}1 < \lambda_2 < 500, \lambda_3 = \lambda_4 = 1, \lambda_4 = \lambda_5 = 0{,}0003$ @ v=108 km/h)

4.4. System Response

After determining weighting coefficients $\lambda_1 - \lambda_5$ frequency and time domain response of the designed system can be obtained. The parameters used in these simulations are the same as listed in Table 3.3. The simulations are realized with the MATLAB.

4.4.1. Frequency domain response

This section presents the frequency response of the vehicle. The bode plots (only magnitude shown) of the controlled system, i.e. the vertical accelerations, the pitch accelerations, the suspension and the tire deflections are illustrated in figure 4.7. The vibration level is closely related to the discomfort of the driver and the passengers.

In these plots, one notices approximate natural frequencies in the 1.59 and 9.54 Hz ranges, or 10 and 60 radians per second on the plot. While the first peak, just above 1 Hz corresponds the natural frequency of the sprung mass (mass mode), the second peak, at the vicinity of 10 Hz represents the natural frequency of the unsprung mass (wheelhop mode).

Human beings are most sensitive in the range specified above and therefore as the ride comfort is concerned it is important to attenuate body acceleration on these frequencies primarily. In fact, vehicle suspensions filter out high frequency inputs, but allow lower frequencies to pass through to the body of the vehicle. Also, human discomfort is known to be most sensitive to vibration in the vertical direction. The driver is placed toward the front of the vehicle, so he is more directly exposed to the front road disturbance.

The reduction in heave and pitch acceleration in the low frequency range corresponds to the increase in the suspension and tire deflections in this range. From the frequency plots for suspension and tire deflections the peaks occur at the two modes of the vehicle, as expected.

On the other hand, one can see that the peak that corresponds to the wheelhop natural frequency is of slightly greater magnitude than the sprung mass mode. This is because active suspension control, in general, does not improve response around the wheelhop frequency. The acceleration responses are close to the passive response at this frequency and they cannot be decreased by feedback. This is largely attributed to the most significant contribution to this mode is tire stiffness, a parameter over which the controller has no control.

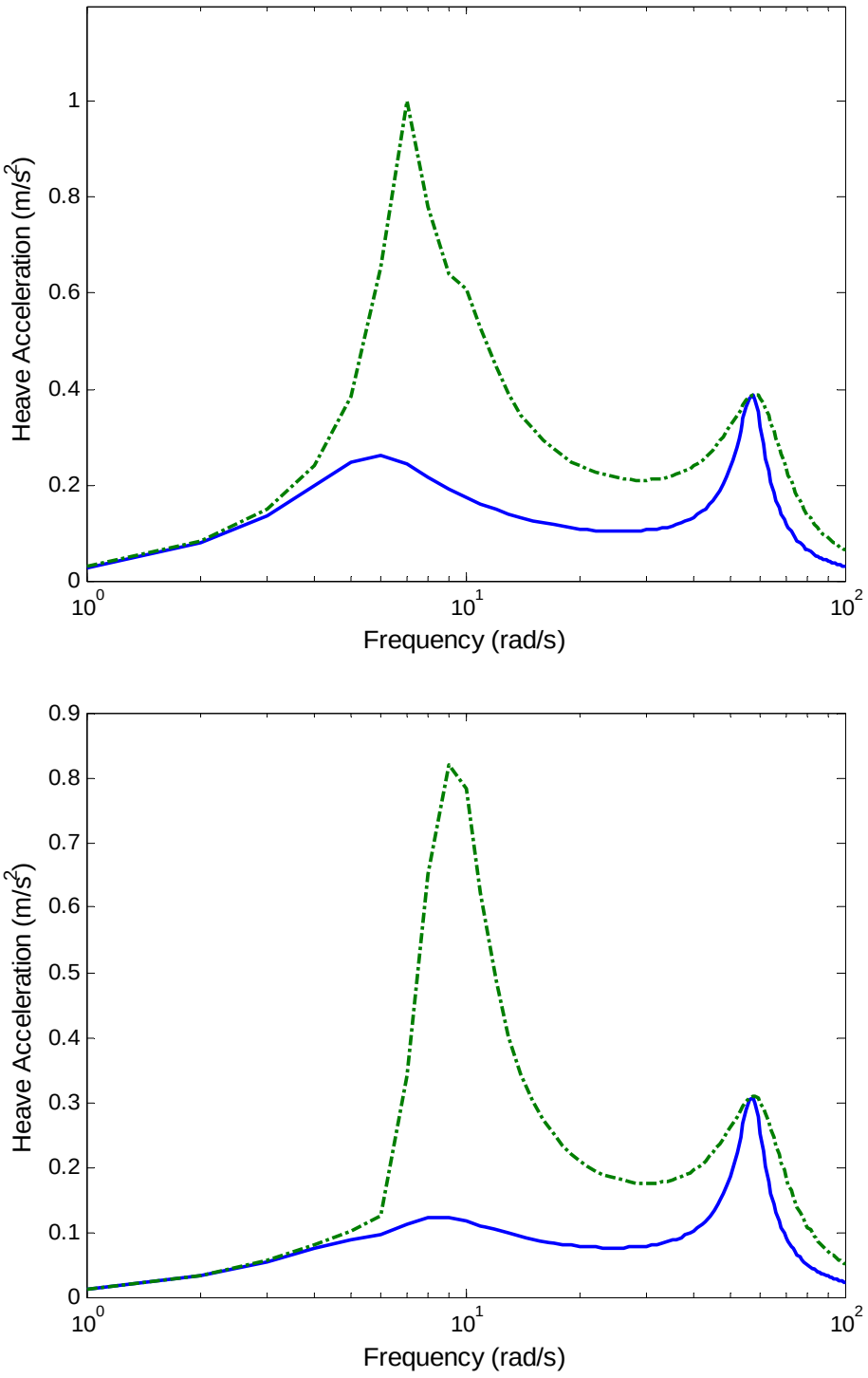

a) Driver seat vertical acceleration. Upper plot for the front road disturbance, below plot for the rear road disturbance. Solid line: active; dash and dots: passive.

Figure 4.7. The frequency response for the actively suspended vehicle to a colored noise ride input @ v= 108 km/h. Solid line: active; dash and dots: passive

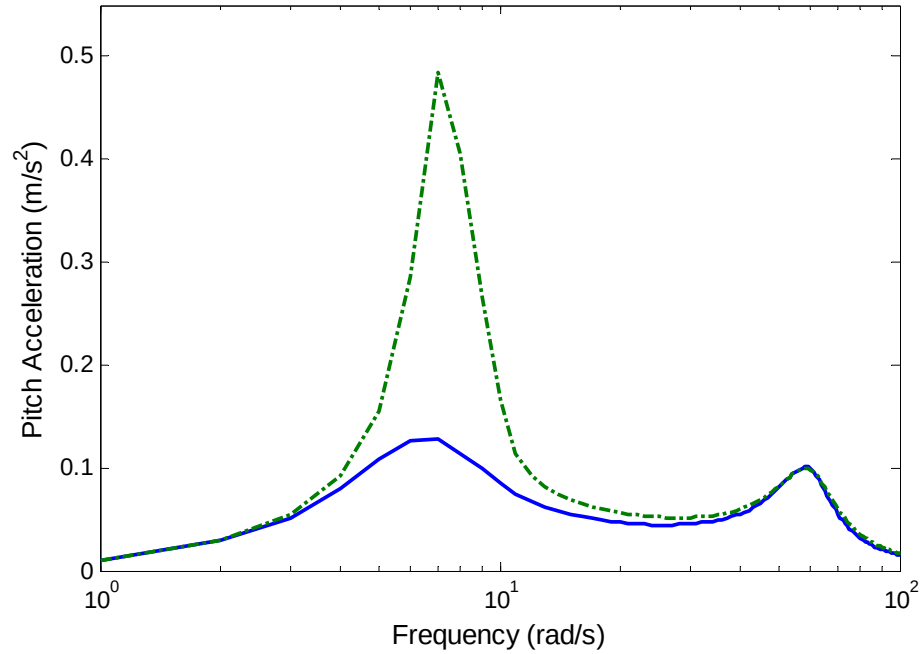

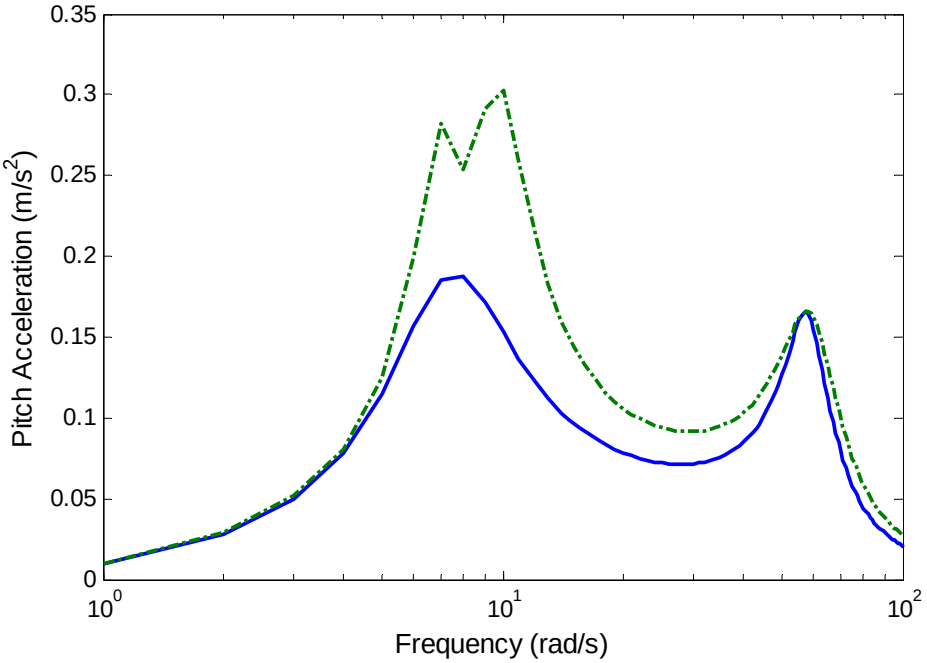

b) Pitch angle acceleration. Upper plot for the front road disturbance, below plot for the rear road disturbance. Solid line: active; dash and dots: passive

Figure 4.7. (Continued) The frequency response for the actively suspended vehicle to a colored noise ride input @ v= 108 km/h. Solid line: active; dash and dots: passive

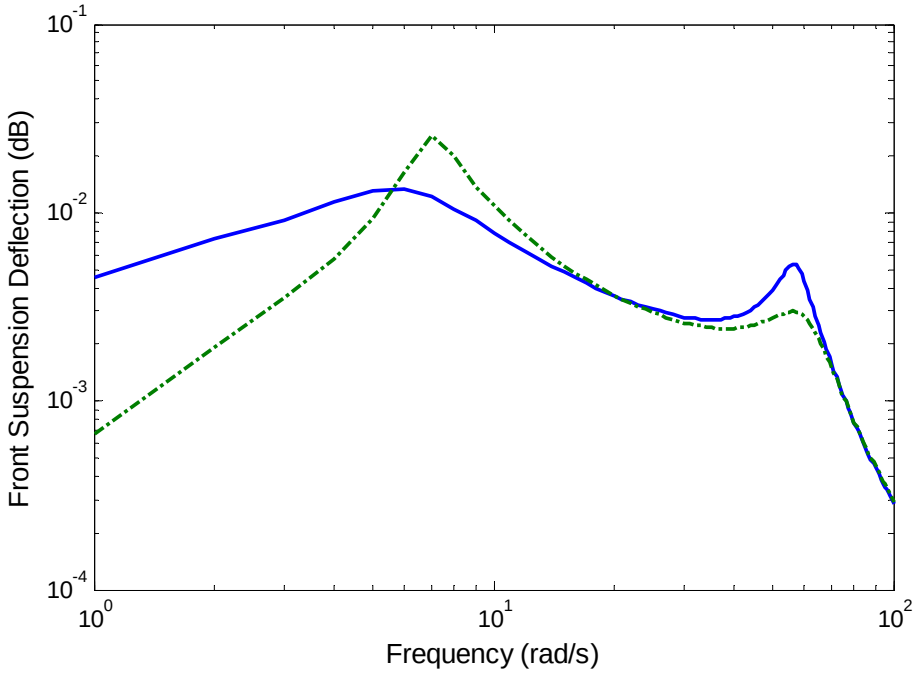

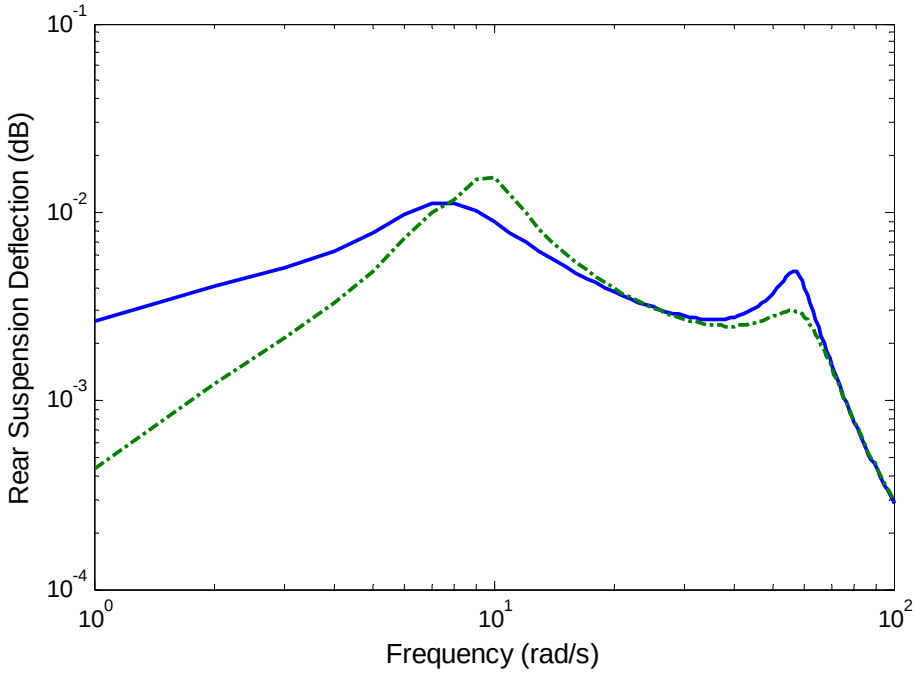

c) Suspension deflection. Upper plot for the front road disturbance, below plot for the rear road disturbance. Solid line: active; dash and dots: passive

Figure 4.7. (Continued) The frequency response for the actively suspended vehicle to a colored noise ride input @ v= 108 km/h. Solid line: active; dash and dots: passive

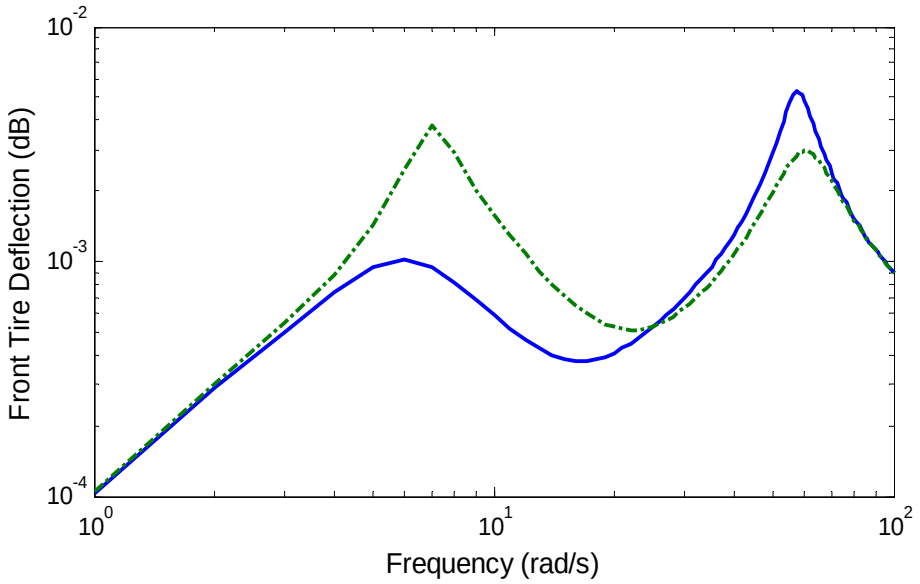

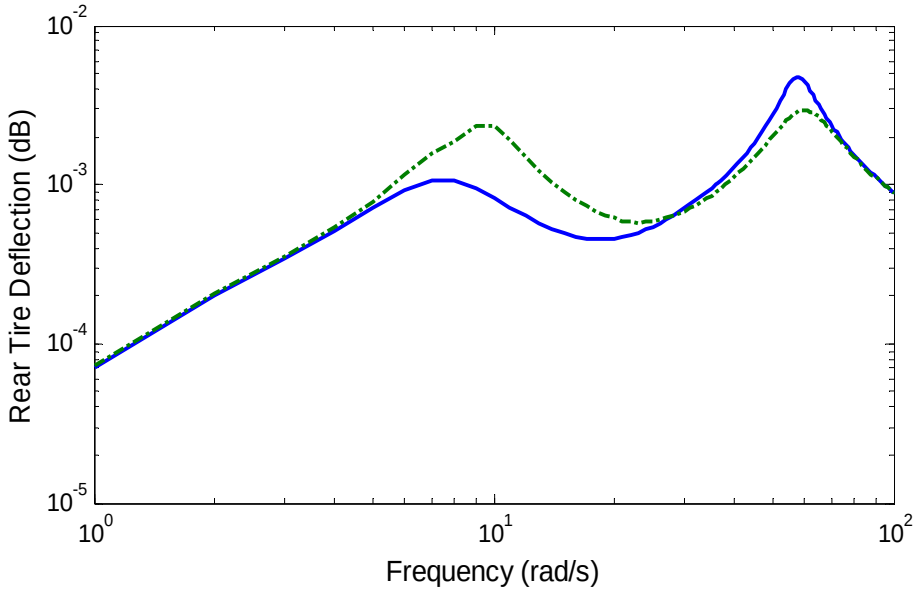

d) Tire Deflection. Upper plot for the front road disturbance, below plot for the rear road disturbance. Solid line: active; dash and dots: passive

Figure 4.7. (Continued) The frequency response for the actively suspended vehicle to a colored noise ride input @ v= 108 km/h. Solid line: active; dash and dots: passive

In order to analyze the results in a different point of view, Table 4.1 below is arranged. In the table, reduction column shows the net RMS reduction of the outputs by the active suspension. Since, passenger comfort in a road vehicle depends on a combination of vertical motion (heave) and angular motions (pitch) the greater importance are given to them.

Table 4.1. RMS values comparison for the design

Regulated Output	**RMS Value (Passive)**	**RMS Value (Active)**	**Reduction (%)**
Driver Seat Vertical Acceleration	2.1884	1.1689	46
Pitch Angle Acceleration	0.8876	0.6462	27
Front Suspension Deflection	0.0291	0.0248	14
Rear Suspension Deflection	0.0244	0.0225	8
Front Tire Deflection	0.0100	0.0127	-
Rear Tire Deflection	0.0098	0.0121	-

On the other hand, Table 4.2 below shows the comparison between passive and active system modes (natural frequencies). Since the system is 4-DOF, two modes for the high frequency (wheel-hop modes) and the other two modes for the low frequency (body modes) totally four modes exist. These modes are deterministic values which are calculated from open and closed system matrices. In the active case, these modes are tried to be reduced.

Table 4.2. Comparison of the system modes

	Passive Case (rad/s)	Active Case (rad/s)
Body Modes	59	57.4
	59,8	58.7
Wheel-Hop Modes	9.4	7.5
	7.1	6.2

4.4.2 Time domain response

It is useful to check the result on the time domain as well. Figure 4.8 shows the random time response of the designed system.

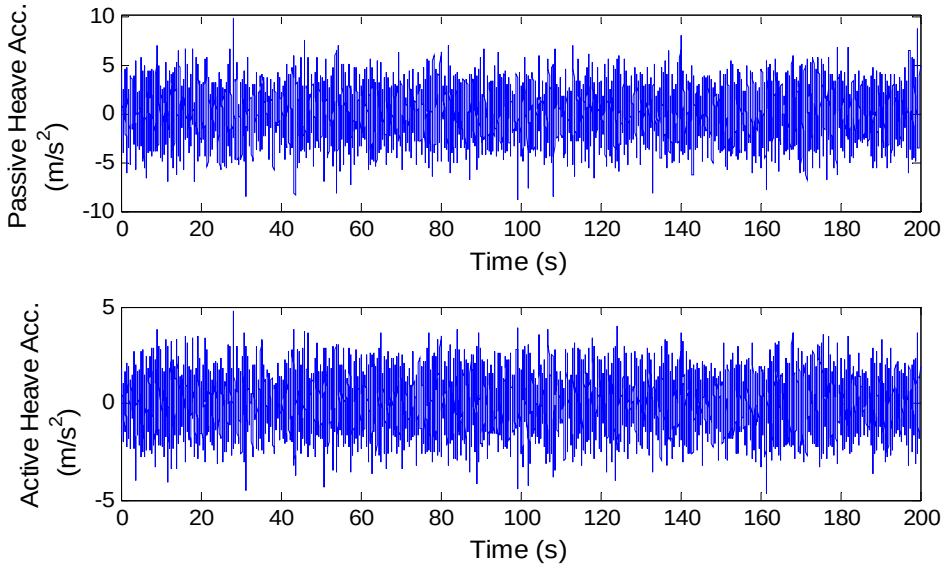

a) Driver seat vertical acceleration. Upper plot for the passively suspended vehicle, below plot for the actively suspended vehicle

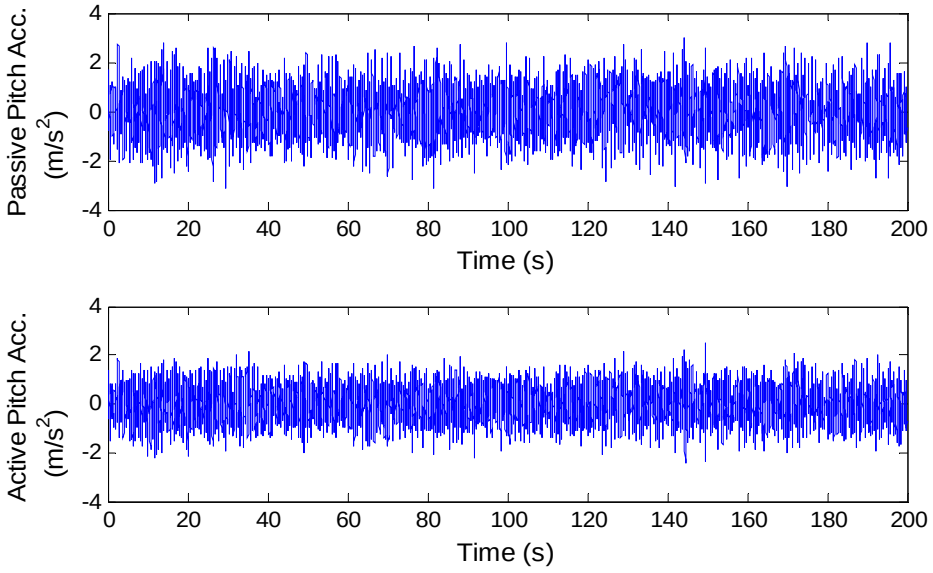

b) Pitch angle acceleration. Upper plot for the passively suspended vehicle, below plot for the actively suspended vehicle

Figure 4.8. Random time response for the actively suspended vehicle to a colored noise ride input @ v=108 km/h

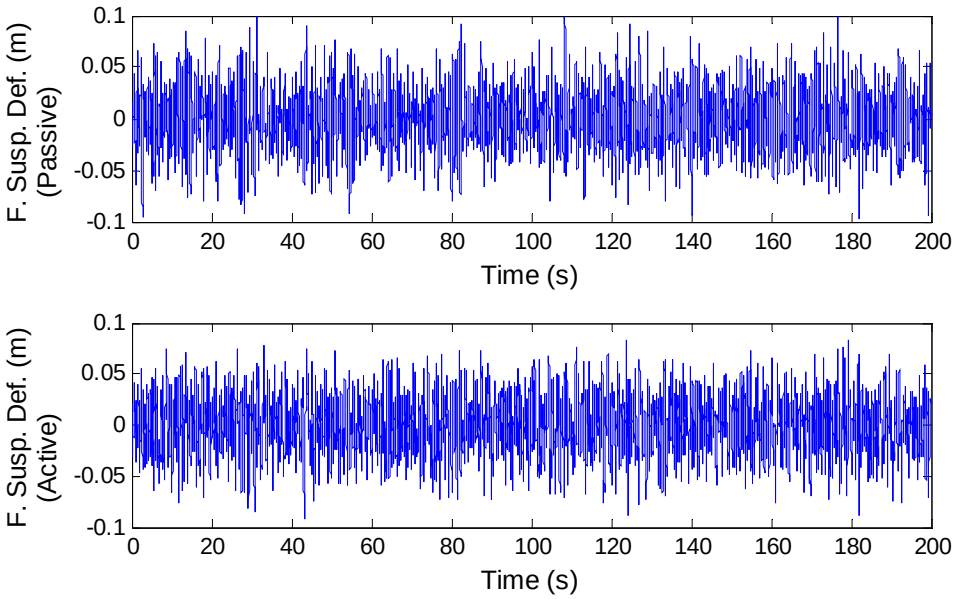

c) Front suspension deflection. Upper plot for the passively suspended vehicle, below plot for the actively suspended vehicle

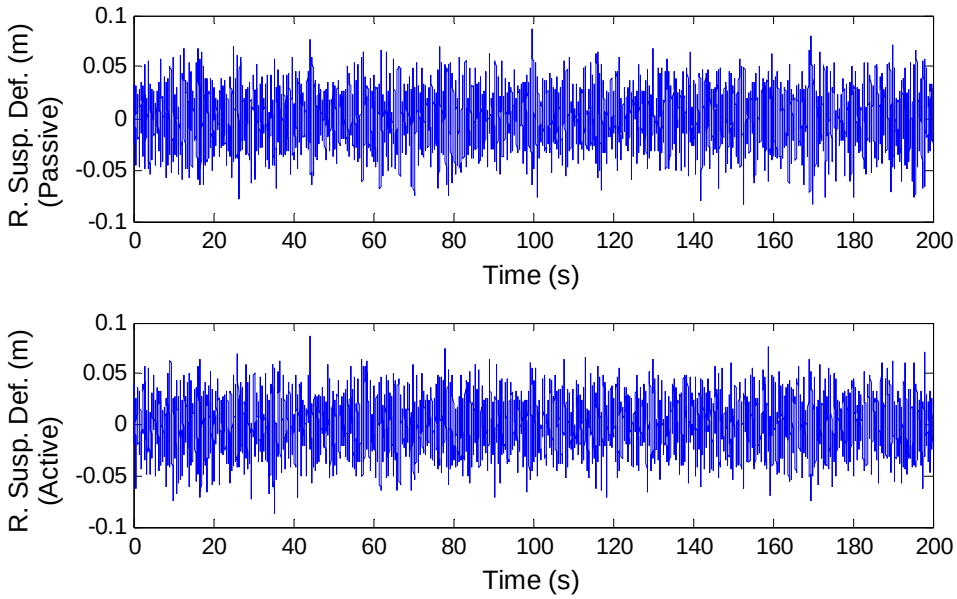

d) Rear suspension deflection. Upper plot for the passively suspended vehicle, below plot for the actively suspended vehicle

Figure 4.8. (Continued) Random time response for the actively suspended vehicle to a colored noise ride input

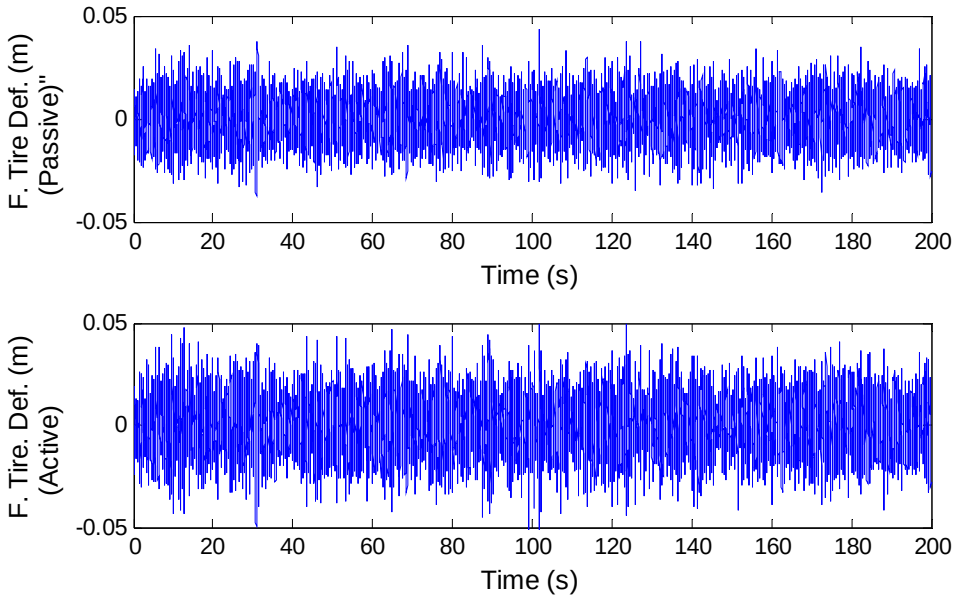

e) Front tire deflection. Upper plot for the passively suspended vehicle, below plot for the actively suspended vehicle

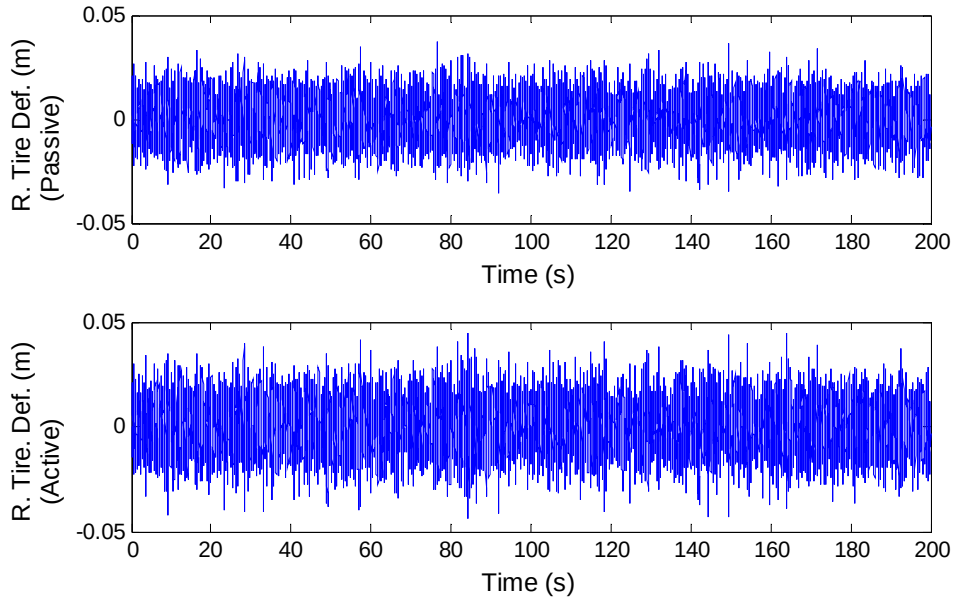

f) Rear tire deflection. Upper plot for the passively suspended vehicle, below plot for the actively suspended vehicle

Figure 4.8. (Continued) Random time response for the actively suspended vehicle to a colored noise ride input

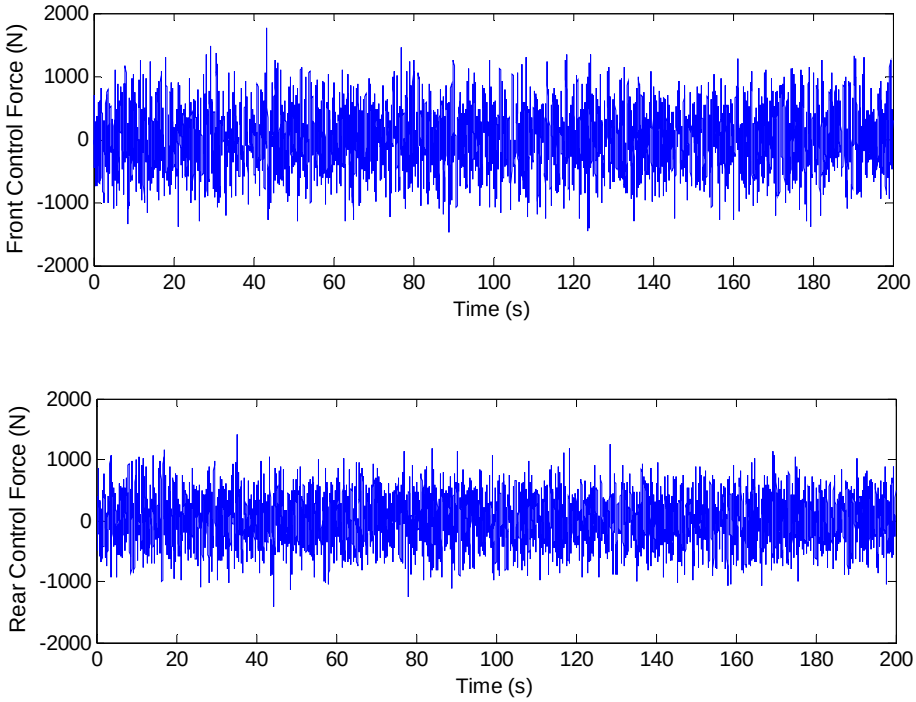

Figure 4.9. Random time response for the actuators

From figure 4.9 it can be observed that control forces are bounded. So far, for the half-vehicle system, random road disturbances are considered. The response of a vehicle to a pothole road input is also discussed and corresponding figures are shown in figure 4.10.

For the all figures shown in this thesis, except the figure 4.10, a fixed vehicle velocity (108 km/h) is considered. However, it is meaningful to investigate the vehicle response for different velocities. Figure 4.11 is plotted in order to observe the system response as a function of vehicle forward velocity. It is shown that deflections and accelerations increase with speed.

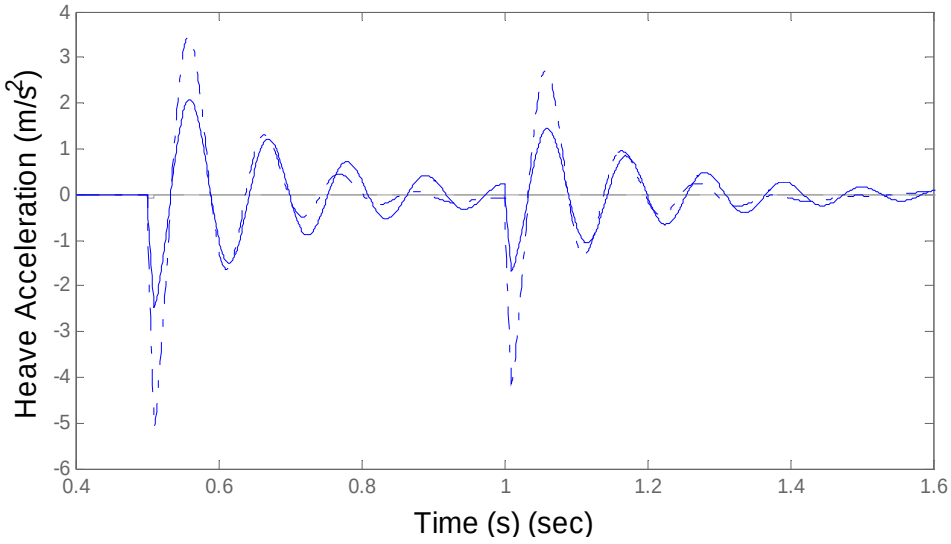

a) Driver seat vertical acceleration. Solid line: active; dash and dots: passive

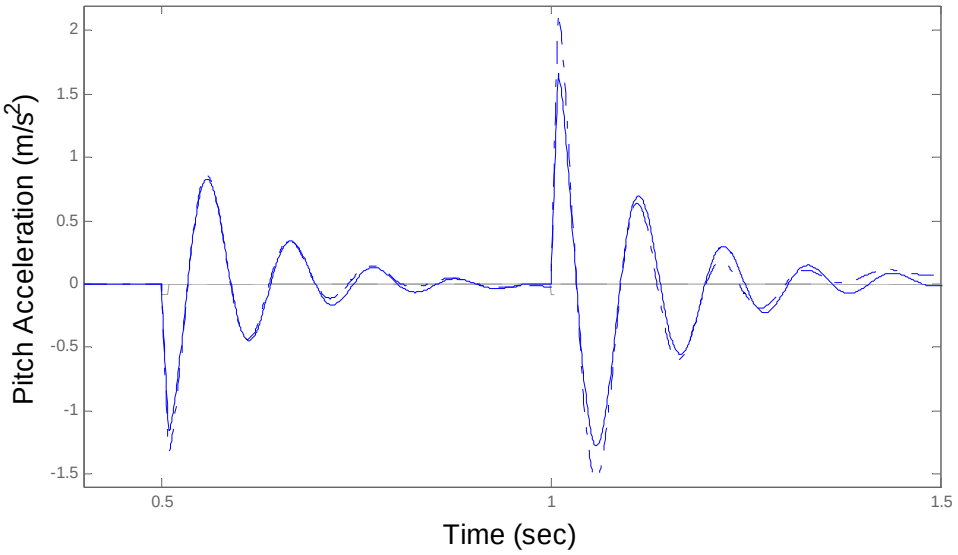

b) Pitch angle acceleration. Solid line: active; dots: passive

Figure 4.10. Comparison of the responses of the actively and passively suspended vehicles when subjected to the pothole type road disturbance
(Solid line: active; and Dots: passive @ v=8 m/s)

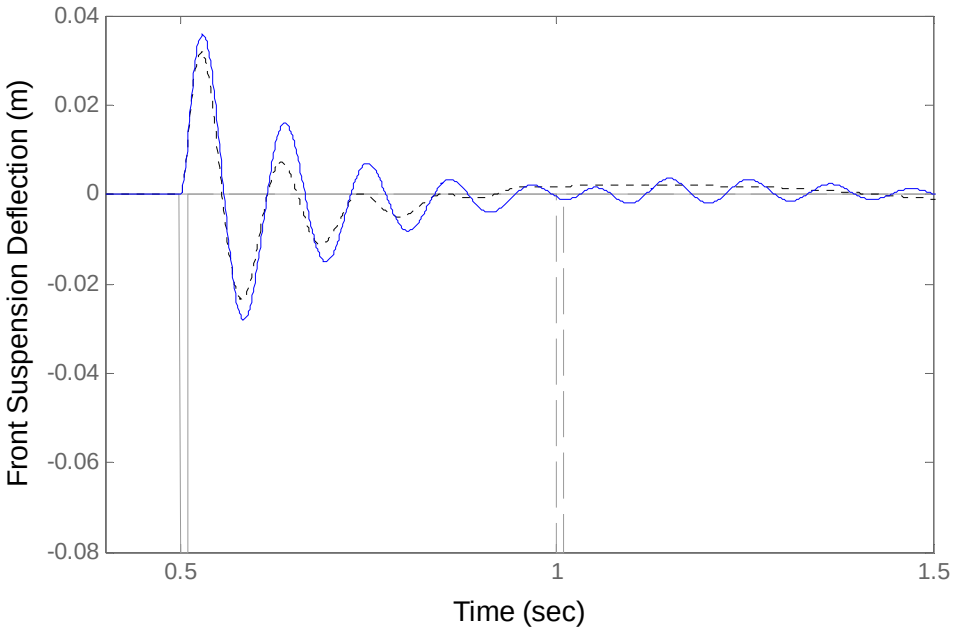

c) Front suspension deflection. Solid line: active; dots: passive

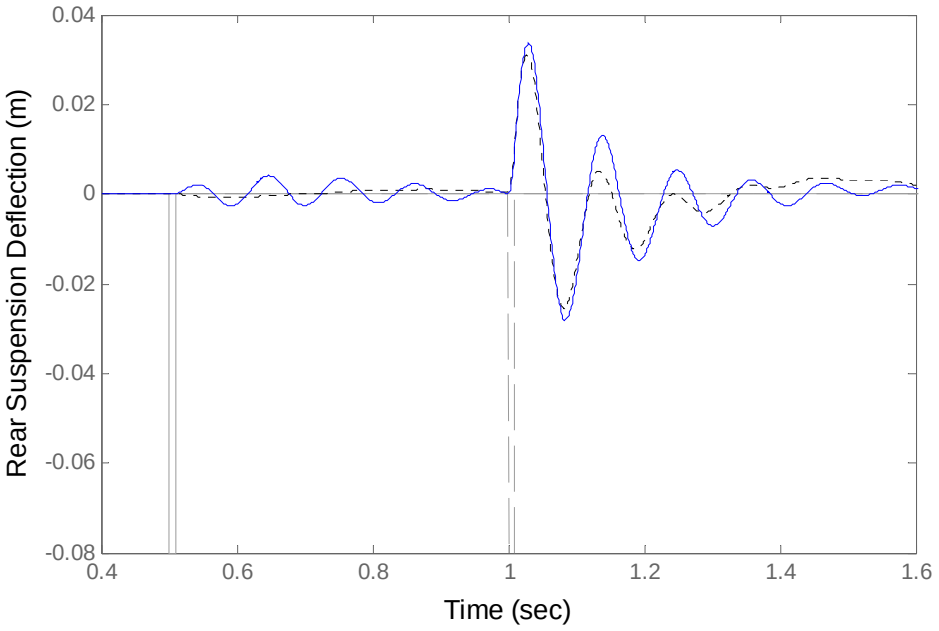

d) Rear suspension deflection. Solid line: active; dots: passive

Figure 4.10. (Continued) Comparison of the responses of the actively and passively suspended vehicle when subjected to the pothole type road disturbance
(Solid line: active; and Dots: passive @ v=8 m/s)

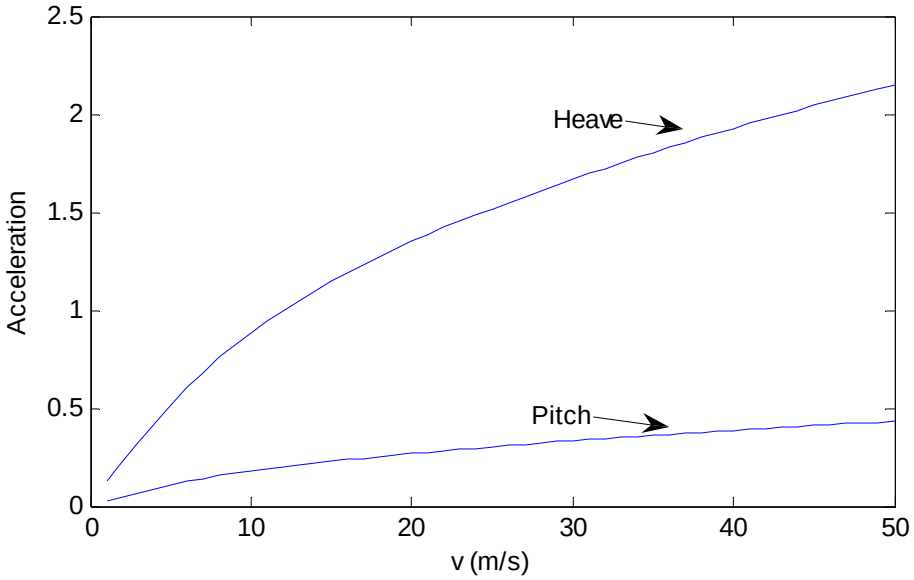

(a)

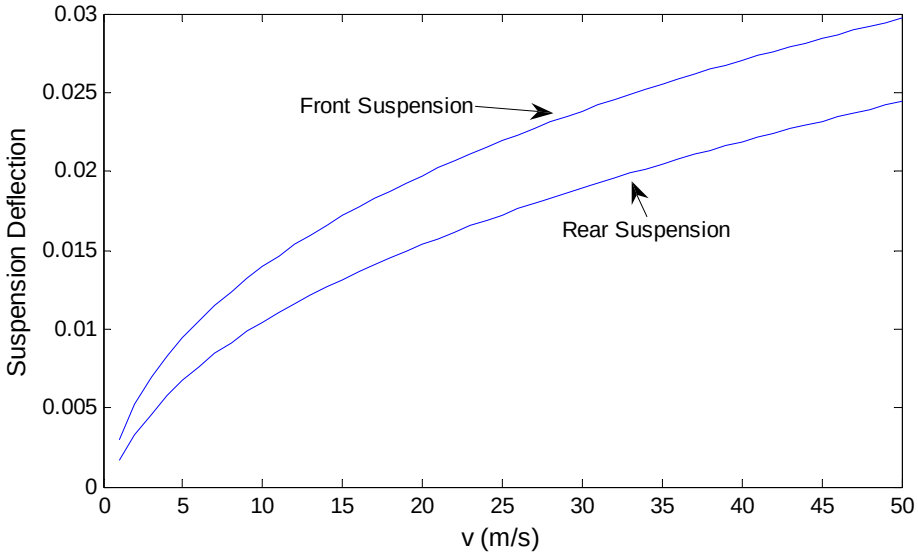

(b)

Figure 4.11. System response as a function of vehicle forward velocity

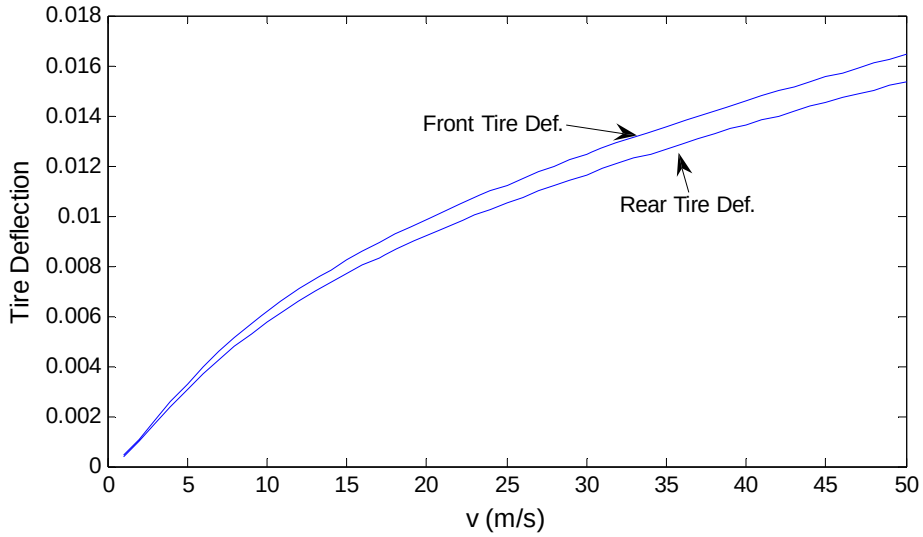

(c)

Figure 4.11. (Continued) System response as a function of vehicle forward velocity

5. CONCLUSION

5.1. Conclusion and Results

In this thesis, a design methodology for active-passive suspension systems was presented for a half-vehicle model. The design procedure is based on the minimization of a quadratic performance index that penalizes the heave, the pitch accelerations and the suspension and tires deformations. By the LQG design, methodology a compensator was designed and its performance characteristics were evaluated.

The road inputs were modeled as the zero-mean colored noise process applied at the input of a linear shape filter whose outputs were derived from the measurements of the road profile power spectrum by an identification algorithm. The Kalman filter was used as an observer to estimate the system states, to make state-feedback implemental.

The performances of the actively suspended vehicle and the passively suspended vehicle system was compared for two kinds of road conditions, namely pothole and random road excitations in terms of the vibration suppression, tire-to-road contact and the demand for rattlespace. RMS responses were computed as well. The simulation results show that an active suspension gives a better performance in terms of ride comfort compared that the passive suspension. An active suspension also increases tire-to-road contact in order to make the vehicle more stable.

More specifically, the simulations in section 4.4 showed that the sprung mass accelerations and unsprung mass displacements of the active system were dramatically smaller than its passive counterpart in the frequency range 1-10 Hz in which the human body is most sensitive to vibration. However, the acceleration attenuation at frequencies of the wheelhop mode are unaffected by the controller. This is because active suspension control, in general, does not improve response around the wheelhop frequency.

For random road disturbances, the proposed full state feedback active suspension reduces RMS sprung mass vertical acceleration around % 46. This ratio is % 27 for the pitch angle acceleration, and nearly 14 %, 8 % for the front and rear suspension travels, respectively.

5.2. Recommendations for Future Work

As a recommendation for the future work, we suggest using a full car model in the design. In this way, a more realistic vehicle model can be proposed. For the road model a simple second order linear shape filter was used in this thesis. Also, higher order shape filters may be used to predict the behavior of the vehicle subjected to random excitations. The system can also be extended to a realistic automobile by adding more DOF's.

REFERENCES

[1] Hrovat, D., *A class of active LQG optimal actuators*, Automatica, **18(1)**, pp. 117-119, Elsevier, Great Britain, 1982.

[2] Krtolica, R., and Hrovat, D., *Optimal active suspension control based on a half-car model: an analytical solution*, IEEE Transactions on Automatic Control, **37(4)**, pp. 528-532, IEEE Control Systems Society, USA, 1992.

[3] Margolis, D.L., and Hrovat, D., "Semi-active heave and pitch control of a high speed tracked air cushion vehicle", *Intersociety Transportation Conference,* Los Angeles-USA, 1976.

[4] Barak, P., and Hrovat, D., "Application of the LQG approach to design of an automotive suspension for three-dimensional vehicle models", *Proceedings International Conference Adv. Suspensions*, ImechE, London, G.B., 1988.

[5] Hrovat, D., and Hubbard, M., "Optimum vehicle suspensions minimizing RMS rattlespace sprung mass acceleration and jerk" *Trans. of the ASME, J. of Dynamic Systems, Measurement and Control*, pp. 228-236, USA, 1981

[6] Chalasani, R.M., "Ride performance potential of active suspension systems Part I: Simplified analysis based on a quarter-car model; Part 1: Comprehensive analysis based on a full car model", *Simulation and Control of Ground Vehicles and Transportation Systems*, *Winter annual meeting of the ASME*, pp 187-234, USA, 1986

[7] Esmailzadeh, E., and Taghirad, H.D., *Active vehicle suspension with optimal state-feedback control,* International of Modeling and simulation, **18(3)**, pp 220-240, USA, 1998.

[8] Hyvarinen, J.P., *The Improvement of Fully Vehicle Semi-active Suspension through Kinematical Model*, Academic dissertation, University of Oulu, 1-157, Finland, 2004.

[9] Bolandhemmat, H.R., Clark, C., "Golnaraghi, "Distributed Sensing System for Vehicles State Estimation." M.F., *Proceedings of The 2006 ASME International Mechanical Engineering Congress and Exposition*, Chicago, Illinois, USA, 2006.

[10] Gillispie, T., *Fundamental of Vehicle Dynamics,* Warrendale, PA: Society of Automotive Engineers, USA, 1992

[11] Alleyne, A. and Hendrick, J., *Nonlinear adaptive control of active suspensions*, IEEE Transactions on Control Systems Technology, **3(1)** , pp. 94-101, USA, 1995

[12] Sampson, D.J.M., *Active Roll Control of. Articulated Heavy Vehicles*, Ph.D. Thesis, University of Cambridge, UK, 2000

[13] Akçay H, Türkay S, *Frequency domain subspace-based identification of discrete-time power spectra from nonuniformly spaced measurements*, Automatica 40, 1333-1347. , Elsevier, Great Britain, 2004

[14] Vessel K.N, *Parametric and Sensitivity Analysis of a Vibratory Automobile Model*, Ms. Thesis, Louisiana State University and A&M College, USA, 2002

[15] Vaughan J.E, *Active and Semi-Active Control to Counter Vehicle Payload. Variation*, Ms. Thesis, Georgia Institute of Technology, USA, 2004

[16] Bowrey, D., Thomas, R., Evans, R. and Richmond, P., *Road humps: Accident Prevention or Hazard?*, Journal of Accident Prevention Hazards, **13**, pp. 288, UK, 1997

[17] Fialho, I.J. and Balas, G.J., *Design of Nonlinear Controllers for Active Vehicle Suspensions using Parameter-Varying Control Synthesis*, Vehicle System Dynamics, **33(5)**, pp. 350–365, Taylor and Francis Ltd, 2000